

Pyroclastic density currents resulting from the interaction of basaltic magma with hydrothermally altered rock: an example from the 2006 summit eruptions of Mount Etna, Italy

B. Behncke · S. Calvari · S. Giammanco · M. Neri ·
H. Pinkerton

Received: 11 June 2007 / Accepted: 31 January 2008 / Published online: 26 April 2008
© Springer-Verlag 2008

Abstract After 16 months of quiescence, Mount Etna began to erupt again in mid-July 2006. The activity was concentrated at and around the Southeast Crater (SEC), one of the four craters on the summit of Etna, and eruptive activity continued intermittently for 5 months. During this period, numerous vents displayed a wide range of eruptive styles at different times. Virtually all explosive activities took place at vents at the summit of the SEC and on its flanks. Eruptive episodes, which lasted from 1 day to 2 weeks, became shorter and more violent with time. Volcanic activity at these vents was often accompanied by dramatic mass-wasting processes such as collapse of parts of the cone, highly unusual flowage processes involving both old rocks and fresh magmatic material, and magma–water interaction. The most dramatic events took place on 16 November, when numerous rockfalls and pyroclastic

density currents (PDCs) were generated during the opening of a large fracture on the SE flank of the SEC cone. The largest PDCs were clearly triggered explosively, and there is evidence that much of the energy was generated during the interaction of intruding magma with wet rocks on the cone's flanks. The most mobile PDCs traveled up to 1 km from their source. This previously unknown process on Etna may not be unique on this volcano and is likely to have taken place on other volcanoes. It represents a newly recognized hazard to those who visit and work in the vicinity of the summit of Etna.

Keywords Mount Etna · Pyroclastic density currents · Lava–water interaction · Hydrothermal alteration · Hazards · Volcano instability · 2006 eruption

Editorial responsibility: JDL White

B. Behncke (✉) · S. Calvari · S. Giammanco · M. Neri
Istituto Nazionale di Geofisica e Vulcanologia,
Sezione di Catania,
Piazza Roma 2,
95123 Catania, Italy
e-mail: behncke@ct.ingv.it

S. Calvari
e-mail: calvari@ct.ingv.it

S. Giammanco
e-mail: giammanco@ct.ingv.it

M. Neri
e-mail: neri@ct.ingv.it

H. Pinkerton
Department of Environmental Science,
Lancaster Environment Centre, Lancaster University,
Lancaster LA1 4YQ, UK
e-mail: h.pinkerton@lancaster.ac.uk

Introduction

Pyroclastic density currents (PDCs) are among the most hazardous of volcanic processes. Because they encompass a wide spectrum of phenomena, dimensions, and genetic mechanisms, different terms are used to describe them. The most commonly used terms for eruption-induced density currents are pyroclastic flows, pyroclastic surges, base surges, glowing clouds or avalanches, nuées ardentes (further distinguished into Merapi-type and St. Vincent-type), ash and block-and-ash flows, and lateral blasts. For more details see Druitt (1998), White and Houghton (2000, 2006), Valentine and Fischer (2000), Freundt et al. (2000), Morrissey et al. (2000), and Branney and Kokelaar (2002). These events are commonly related to explosive eruptions (eruption column collapse) and extrusion of viscous lava (dome or lava flow collapse).

An additional range of processes that form fragmental deposits on volcanoes include rockfalls, rockfall avalanches, lahars, and debris avalanches (Vallance 2000; Ui et al. 2000). While some of these events are triggered by eruptive activity, others arise as a consequence of gravitational instability, seismicity, and/or interaction with external water (which may be hydrothermal, phreatic, or meteoric).

According to Tanguy et al. (1998), nearly 44% of the total number of fatalities on or around volcanoes between 1783 and 1997 were the result of PDCs and lahars. During the twentieth century, this increased to more than 80% (Witham 2005). This trend is confirmed by recent volcanic events in 2006 (pyroclastic flows at Merapi in Indonesia and Tungurahua in Ecuador, and post eruptive lahars at Mayon in the Philippines; CVGHM 2006; IGEPN 2006; ReliefWeb 2006–2007).

Such problems are generally of little concern to the population living near Mount Etna in Sicily (southern Italy; Fig. 1) where the greatest hazard arises from lava flows (Behncke et al. 2005) released from vents on the flanks close to densely populated areas as happened in 1669 (Corsaro et al. 1996; Crisci et al. 2003) and again in 1928 (Duncan et al. 1996). Although potentially highly destructive, lava flows at Etna generally move slowly and thus do not represent a direct threat to human lives. All historically known eruption-related fatalities at Etna were caused by (minor) explosive eruptions or lava–water interaction (Chester et al. 1985; Gemmellaro 1843; Haeni 1931; Kieffer 1979, 1982; Guest et al. 1980; Murray 1980). The number of confirmed eruption victims for this volcano during the past 2000 years is <80.

Etna has produced no major explosive eruptions, pyroclastic flows, and/or lahars within living memory, leading to the widespread belief that it is essentially a nonexplosive volcano. However, Etna generated voluminous pyroclastic flows during a series of climactic explosive eruptions about 15,000 years ago (De Rita et al. 1991), and minor PDCs occurred repeatedly during the past few tens of millennia, including the Plinian 122 BC eruption (Coltelli et al. 1998). Small pyroclastic flows were observed during a violent explosive episode at the Northeast Crater (one of Etna's four summit craters; Fig. 1b) in 1986 (Murray et al. 1989–1990; P. Allard, personal communication 2006). More recently, pyroclastic flows and other density currents and/or rockfalls and avalanches occurred at Etna's summit craters in 1999 (Calvari and Pinkerton 2002; Harris and Neri 2002; Behncke et al. 2003) and 2000 (Tanguy, personal communication 2006). Modest-sized PDCs were again observed on several occasions during the 2006–2007 summit eruptions. While not dangerous for those living on the lower flanks, these density currents affected areas frequently visited by tourists (several hundreds to thousands per day during the summer season,

which lasts from May to October). These observations led to a heightened awareness of the possibility of hazardous mass flowage processes when activity resumed at the summit during the summer of 2006. Between then and mid-December 2006, there was a complex sequence of eruptions at and near the Southeast Crater (SEC; Fig. 1b), the youngest and most active of Etna's summit craters.

In this paper, we summarize the main characteristics of the 2006 summit eruptions before discussing in more detail the various collapse and flowage events that occurred during this eruptive period. We concentrate in particular on a dramatic eruptive episode on 16 November. We use a combination of direct observations, photography, and video footage made by ourselves, our colleagues, and other eyewitnesses to reconstruct and interpret the sequence of events of that day, and we conclude with a reappraisal of volcanic hazards in the summit area of this volcano.

Terminology

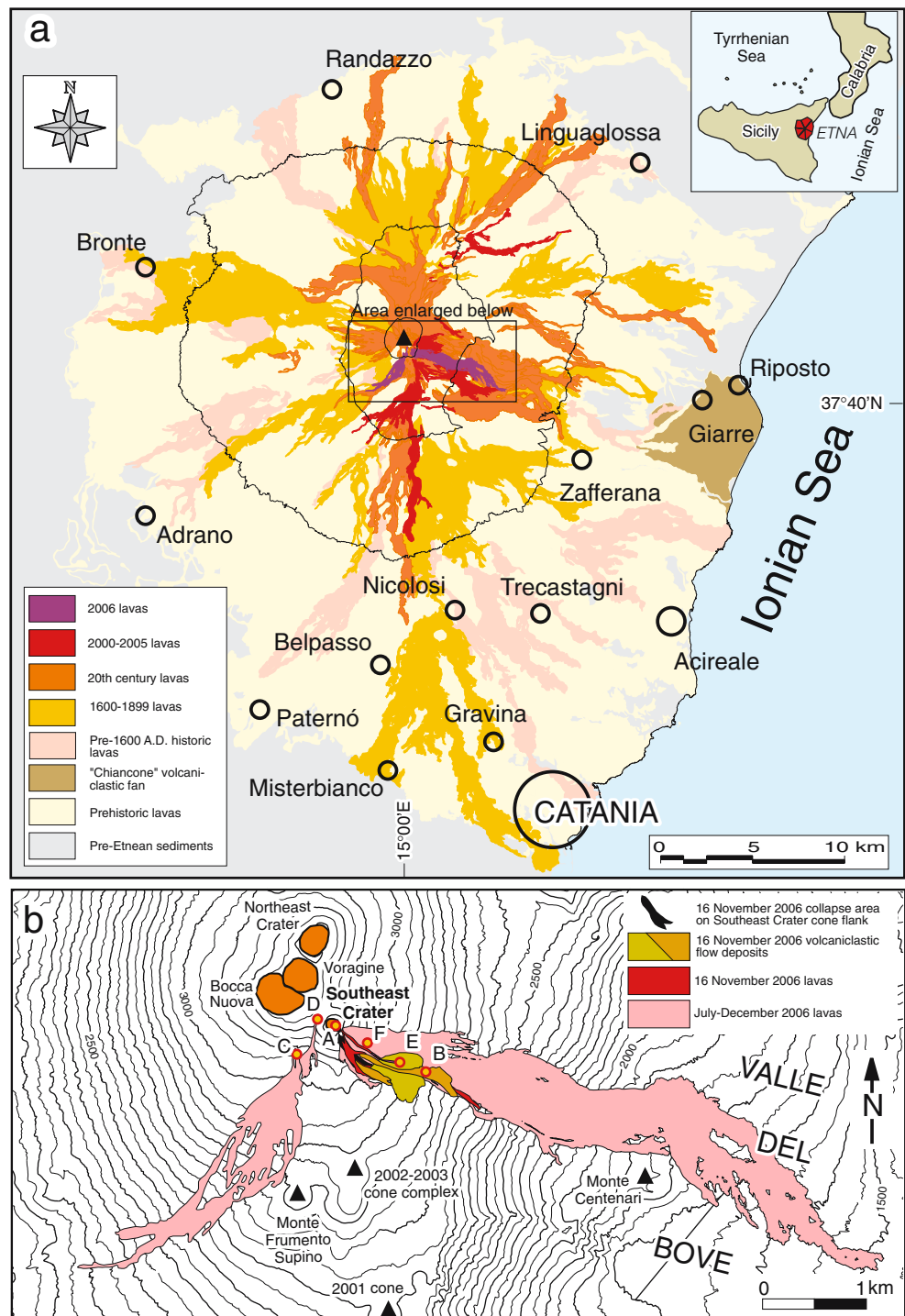
One problem we encountered during the analysis of the events described in this paper is the volcanological terminology used to describe explosively generated volcanoclastic density currents. It has become widespread usage to call all kinds of ground-hugging, more or less explosively induced density currents “pyroclastic,” including base surges created by the interaction of magma with external water (e.g., Brand and White 2004)—which *sensu stricto* is not a pyroclastic, but a hydroclastic mechanism. In spite of these reservations, we adhere to the commonly used terminology and apply the term “pyroclastic density currents” in a generic sense, and more descriptive expressions such as “ground-hugging ash and vapor clouds,” “rockfalls and rock avalanches” or other similar terms where these terms more accurately reflect the processes that are taking place at the time of their formation.

The 2006 summit eruptions: an overview

Sixteen months after the end of the 2004–2005 flank eruption (Burton et al. 2005; Neri and Acocella 2006), Etna entered into a new period of summit activity in mid-July 2006 (Neri et al. 2006), and this continued intermittently for 5 months. Activity was concentrated in vents at and around the SEC at different times (Fig. 1b). A schematic timeline of the 2006 activity is shown in Fig. 2.

The 2006 eruption was characterised by two main phases of activity. The first lasted from 14 to 24 July when Strombolian and effusive activity took place along a short fissure on the lower ESE flank of the SEC cone. This phase culminated with a short episode of lava fountaining on 20

Fig. 1 **a** Overview map of Mount Etna showing the distribution of prehistoric and historic lavas including those of 2006 and locations of selected towns near Etna. *Inset at upper right* shows the regional context of the Etna area. **b** Map of the 2006 eruption area, vents, and lava flows. *A* summit vent of the Southeast Crater, *B* vent at 2,800 m asl, *C* vent at 3,050 m asl, *D* vent at 2,180 m asl, *E* vent at approximately 3,100 m asl that was active on 30 November–3 December 2006, *F* pit crater formed on 23 October 2006 and site of Strombolian activity and ash emissions in early–mid-December 2006



July. The second phase lasted from 31 August until 14 December (Calvari and Behncke 2006, 2007; Calvari et al. 2006). It consisted of 20 eruptive episodes at or near the summit of the SEC cone (vent "A" in Fig. 1b), accompanied, from 12 October onward, by periodic effusive activity from a number of vents at various sites to the E–SE and W–SW of the cone (Fig. 1b).

The most persistent effusive vents formed on 12 and 26 October. The former lay at 2,800 m asl on the upper W wall

of the Valle del Bove, about 0.9 km SE of the SEC (vent "B" in Fig. 1b); the latter opened at 3,050 m at the S base of the Bocca Nuova, about 0.45 km from the SEC (vent "C" in Fig. 1b). While vent "B" remained continuously active throughout early December, vent "C" tended to erupt mainly during paroxysmal episodes at the SEC and shut down on 24 November.

Other effusive vents were intermittently active on the W, E, S, and SE flanks of the SEC cone (vents "D," "E," and

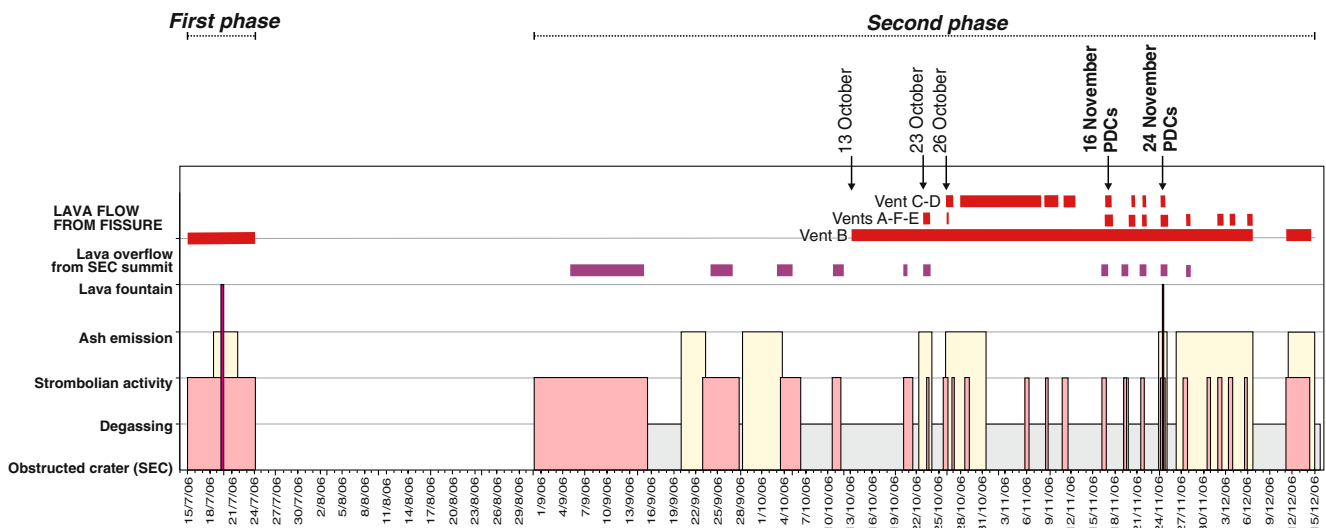


Fig. 2 Timeline of the 2006 Southeast Crater eruptions, distinguishing different eruptive styles and periods of activity of the different vents as described in the text (for locations, see Fig. 1b). The dates of

“F” in Fig. 1b). After a final vigorous burst of activity from vents at the E side of the SEC and from vent “B,” the activity stopped abruptly on 14 December. Maximum lava flow lengths during the 2006 eruptions were 3.9 km (July eruptive phase), 4.8 km (vent “B”), and 3.5 km (vent “C”) (Fig. 1b). The total volume of lava erupted during the 2006 activity is estimated at $15\text{--}20 \times 10^6 \text{ m}^3$.

The Southeast Crater before the 2006 eruptions

Much of the present-day SEC edifice is a steep-sided cone that was built up between 1978 and 2001, rising to a height of approximately 250 m above its base (Calvari et al. 1994a; Behncke et al. 2006). The upper portion of the cone was constructed during numerous short-lived episodes of lava fountaining and consists of more or less agglutinated spatter, loose scoria, and a minor proportion of rootless lava flows.

The symmetrical shape of the cone was broken during a nearby flank eruption in late 2004 to early 2005 when a circular collapse pit formed on the upper ESE flank of the cone (Neri and Aocella 2006). During that eruption, the pit gradually enlarged to a final diameter of approximately 250 m and periodically emitted lithic ash, probably as a result of the foundering of the conduit walls during the emptying of a reservoir located below the SEC. After the end of the eruption, the pit was partially filled by collapse deposits, its depth decreased, and the upper (WNW) rim began to bite into the rim of the summit crater of the SEC. As a consequence, a thin septum with an irregular, craggy rim was left between the summit vent and the 2004–2005 pit (Fig. 3a).

The first phase of the 2006 summit activity (in July) took place below the lower (ESE) rim of the 2004–2005 collapse pit (Fig. 3a), whose morphology—as that of the remainder

opening of the main effusive vents and the major pyroclastic density current-producing events are highlighted

of the SEC cone—did not undergo any notable morphological changes. In contrast, the second phase of activity started at the summit vent of the SEC, very close to the thin septum separating it from the adjacent pit.

At the time of the 2006 summit eruptions, large portions of the southern and eastern flanks of the SEC cone had become unstable, partly due to the formation of the 2004–2005 collapse pit. In addition, hydrothermal activity had

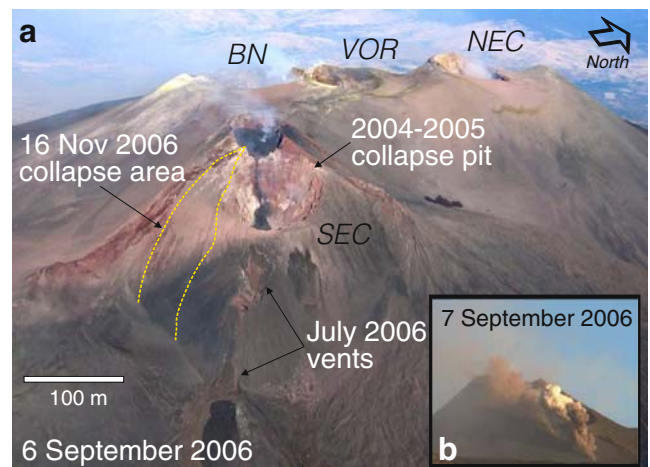


Fig. 3 **a** WNW-looking aerial view of the summit area of Etna on 6 September 2006, showing the Southeast Crater in the foreground. Significant features (2004–2005 collapse pit, July 2006 vents and 16 November 2006 collapse area) are indicated. Photo from the digital image collection of the Catania Section of the Istituto Nazionale di Geofisica e Vulcanologia. **b** Scene captured by a time-lapse camera at Schiena dell’Asino (approximately 5 km SE of the Southeast Crater) on the morning of 7 September 2006. Lava fed from the summit of the Southeast Crater cone plunges into one of the July 2006 vents, generating collapse (brown ash plumes) and interacting with moist rocks (white vapor plumes). Similar plumes were seen during the previous days when lava flowed across the upper and lower rims of the 2004–2005 collapse pit. Image courtesy of Etnatrekking

continued ever since the temporary cessation of eruptive activity in 2001, causing pervasive alteration of the flanks. Such a condition has been recognized as capable of rendering a volcano more prone to collapse (Lopez and Williams 1993; Reid et al. 2001; Zimbelman et al. 2004; Opfergelt et al. 2006), and indeed, it played a determining role in the events described in the following sections.

Minor collapse events, September 2006

While the first (14–24 July; Neri et al. 2006) phase of activity was not accompanied by significant collapse and flowage events, such phenomena became a fairly common feature during many of the eruptive episodes of the second phase, starting in early September.

The first observed collapse event occurred on the evening of 4 September, 5 days after eruptive activity resumed at the summit of the SEC. Initially, this activity consisted of very weak Strombolian explosions, but on the evening of 4 September, lava began to flow over the craggy and unstable E rim of the crater and cascade into the adjacent 2004–2005 collapse pit (Fig. 3a). The onset of lava effusion was preceded by the sudden release of a series of ash and vapor plumes from the E side of the SEC cone, and these were recorded by the INGV-CT monitoring cameras. The ash and vapor plumes were generated during the collapse of a portion of the near-vertical wall of the 2004–2005 pit (see the “Discussion” section for an interpretation). Some of the collapsed material descended well beyond the lower rim of that pit and beyond the base of the SEC cone.

During the following days, lava gradually filled the bottom of the pit, raising it toward the lower ESE rim. During the morning of 7 September, the rim failed during a series of collapses, which, like those 3 days earlier, generated rock avalanches that descended rapidly to a distance of several hundred meters from the base of the SEC cone. These collapses were also accompanied by white vapor plumes (Fig. 3b). After this, lava began to flow through the breach and then covered the explosive vents of the July 2006 eruptive phase, each time provoking another series of rockfalls and avalanches. Thereafter, however, the situation gradually stabilized and no significant collapse and/or PDCs were observed during a number of eruptive episodes from the SEC through mid-November.

Volcanic activity on 16 November 2006

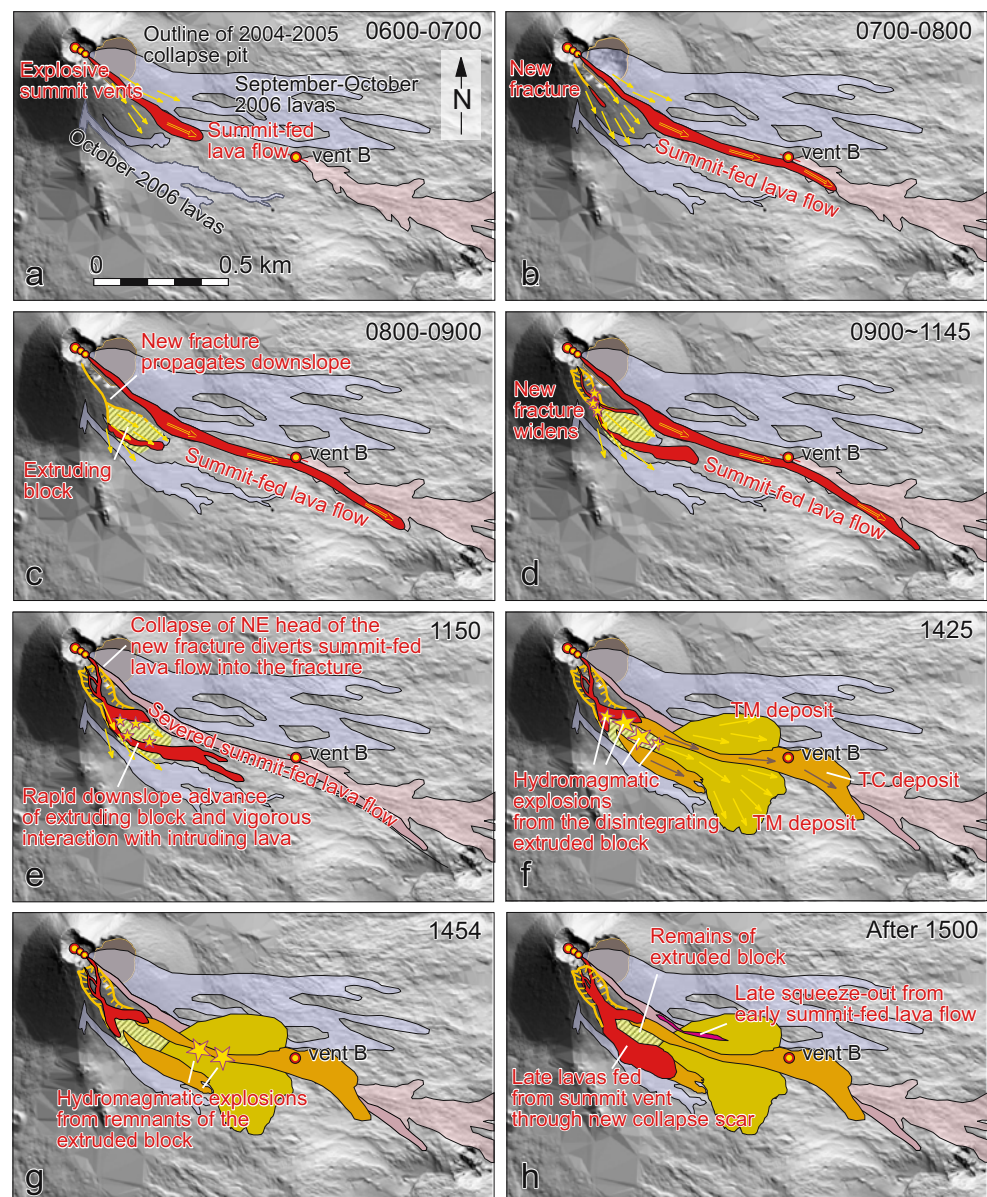
The eruptive episode on 16 November 2006 started shortly after 0500 GMT with Strombolian explosions from the summit of the SEC, followed, about 1 h later, by lava emission from a vent on the SE side of the summit area

(Fig. 4a). The lava flowed across a series of craggy and strongly altered remnants of the SW rim of the 2004–2005 collapse pit. As the lava bulldozed over and through this highly unstable area, it triggered a series of rockfalls accompanied by steam and dust plumes. The lava flow then advanced approximately 1.2 km toward the Valle del Bove during the next few hours (Fig. 4b).

A new fracture began to open on the upper SSE side of the cone around 0700 (Fig. 4b). This fracture widened and propagated downslope during the next few hours, and this was accompanied by dense steam emissions, very frequent rockfalls, and avalanches of rock debris mixed with fresh lava that issued from various points along the fracture. For a brief period, lava issued from the lower termination of the fracture when it was still three quarters of the way up the slope, and there was strong interaction with the moist rock upon which it flowed. Observers describe a process that resembled boiling, which produced steam plumes and led to the disintegration of both the hot lava and the underlying rocks, generating rock avalanches that cascaded down the slope. At first, these avalanches traveled only for short distances, but eventually they reached the base of the cone as the explosive interaction intensified and its focus shifted downslope. This process initiated channel erosion of the cone along the path of the lava flow. Continued erosion along the propagating fracture deepened and widened this channel, which gradually evolved into a deep scar on the cone’s flank.

Direct observation by the authors began around 0815 GMT. At this time, nearly continuous Strombolian explosions were taking place at the summit of the SEC cone, while nearby vents (further to the east) produced mainly ash and sporadic ejections of large bombs. Lava continued to be erupted from the summit down the south–east flank and from a vent at the head of the new fracture. By the time our first observations were made, this had developed into an impressive scar, whose sides were subject to frequent collapse. At its lower end, the fracture bifurcated around a block of the lower flank of the SEC cone, in the shape of an inverted Y (Fig. 4c). The block delimited by the two branches of the fracture was highly mobile and protruded out of the side of the cone, its front crumbling almost constantly, and vapor issuing from numerous points on the block’s surface. At the same time, lava emerged from the lower terminations of the fracture on both sides of the extruding block (Fig. 4d). The discharge rate of lava from the fracture was pulsatory and resulted in surges of very fast-moving lava flows which transported abundant blocks of light-colored altered old material. Each surge was preceded by emissions of dense white steam plumes from within the fracture (locations indicated by yellow asterisks in Fig. 4d), and these were frequently accompanied by low tephra fountains that sometimes seemed to “boil” over a place before collapsing and spilling rapidly downslope in a

Fig. 4 Maps showing the evolution of lava flows, fractures, and pyroclastic density currents during the 16 November 2006 eruptive episode. Flow directions are indicated by arrows; yellow asterisks indicate the sites and magnitude of hydro-magmatic explosive activity. Digital elevation model (updated to 2005) used as base courtesy of M.T. Pareschi, INGV-Pisa

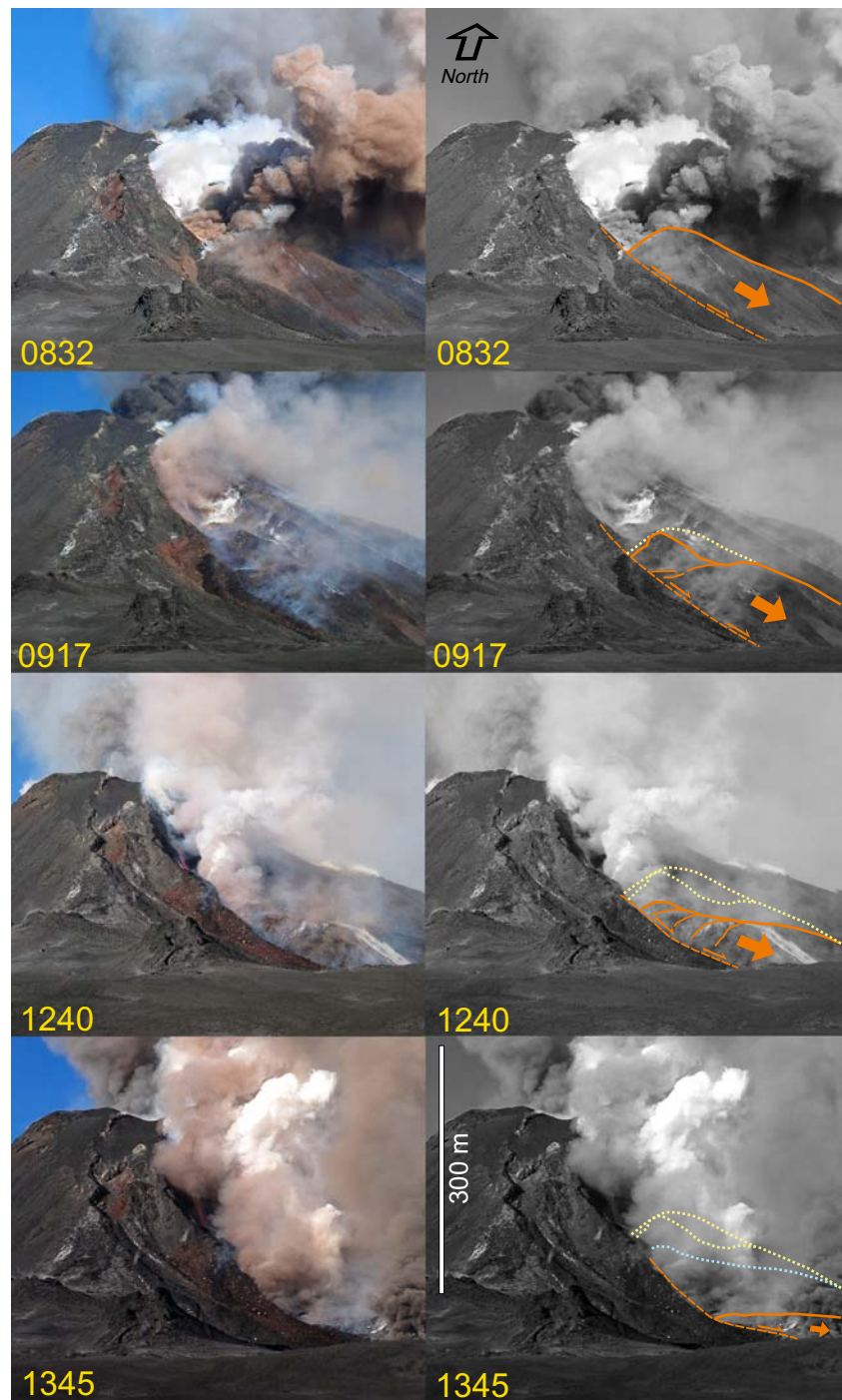


manner that closely resembled the advance of pyroclastic flows. Most of the larger clasts thrown up with the tephra fountains appeared to be lithic material, at times producing distinct vapor trails. Occasional views of the basal portions of the ground-hugging ash clouds revealed them to consist of avalanches of rock fragments mixed with incandescent lava. Most of these avalanches were confined to the lower portions of the SEC cone, but a few of the larger avalanches traveled 100–200 m beyond the base of the SEC (see yellow arrows in Fig. 3d).

By 1150, the combination of lava–wet rock interaction, gravitational instability, and erosion by lava had created a deep scar in the SE flank of the SEC cone (Figs. 4e and 5). Lava emerging from a vent high in the headwall of the scar formed a spectacular cascade several tens of meters high. Lava also issued from the lower termination of the scar,

which, by this time, had eroded downslope nearly to the base of the cone. Collapse of the upper rims of the scar had progressed, eroding into the adjacent portions of the flank toward the active lava flow on the ESE side of the cone. A time series of thermal images show that a major change took place at 1150 GMT. The large summit lava flow that descended down a channel on the northerly side of the breach in the SEC was severed and diverted into the scar, so that a second cascade formed within this large collapse feature (Fig. 4e). This lava flow cascaded down toward the unstable block. The beheading and diversion of the lava flow was accompanied by several minutes of intense PDC activity and by the production of large plumes of white vapor. After this, periodic emissions of white vapor, rockfalls, and rock–lava avalanches with rolling ash clouds continued to issue from various portions of the breach.

Fig. 5 Comparison photographs taken at different times from the same viewing point on 16 November 2006, showing progressive outward and downward movement of the block pushed out of the lower SE flank of the Southeast Crater cone. Time indicated in GMT. Frames in right column highlight changing position and shape of the block. View is from about 1 km south of the summit of the Southeast Crater. Note flattening out of the block at the base of the cone and ash plumes rising from several spots on the block in last (1345 GMT) frame. Photo in last frame courtesy of Nino Mazzaglia



At this time, the remainder of the protruding block at the base of the SEC cone was reduced to a relatively flat, broad hill (Fig. 5, 1345 frame). It was extremely mobile with material crumbling constantly from its sides and vapor and occasional ash emissions from various spots. Incandescent lava was extruding in places from the surface of the block. A major collapse occurred within the breach at 1345 GMT and produced a large mixed ash–vapor plume.

At 1425 GMT, a major explosive event occurred from an area at the base of the SEC cone, generating the PDCs of the 16 November eruptive episode; a somewhat smaller explosion at 1455 GMT occurred from a location still farther from the SEC cone (Fig. 4f–g). These events are described in detail in the next section.

After 1500 GMT, activity continued much the same as before with Strombolian explosions from the uppermost

summit vent and continued ash and bomb emission from the two nearby vents. The main difference was that lava now flowed entirely through the deep incision in the SE flank of the cone, forming numerous spectacular cascades. Small- and medium-sized collapses, rockfalls, and avalanches continued throughout the late afternoon. Around 1600 GMT, explosive activity gradually subsided, but lava continued to cascade through the collapse scar until late that night (Fig. 4h).

The culminating events

At 1424 GMT on 16 November, a jet of light brown ash and large, nonincandescent clasts began to spurt from the lower end of the mobile block, followed 10–15 s later by the ejection of a similar spray a few tens of meters further to the W (toward the SEC). For a brief period, the activity migrated from one spot to another and then extended to more and more points. The only audible noise was the clattering of large rock fragments as they fell back on the ground.

Within about 1 min (at 1425 GMT), dark vertical tephra jets rose from several points aligned along what seemed to be a radial fracture opening at the SE base of the SEC cone (Fig. 6). The jets ejected abundant bombs and boulders, none of which appeared to be incandescent; many were followed by vapor trails (see enlargements in Fig. 6). Within a few tens of seconds, the jets became broader and

darker material was emitted, forming cypressoid (cock's tail) plumes that rose a few tens of meters above the ground before collapsing and spreading laterally and downslope. Simultaneously, voluminous plumes of white vapor were emitted. The line of emission points seemed to propagate both downslope and upslope like an opening eruptive fissure. At the same time, a massive collapse occurred within the scar formed in the cone's SE flank during the previous hours, producing a reddish-brown cloud (Fig. 7a).

A few moments later, a large white steam plume rose from the area, expanding both upward into the sky and downslope toward the E (Fig. 7b, c). Dark material then began to appear at the base of the white plume, which likewise expanded both vertically and downslope. The dark density current soon overrode the white plume, and both disappeared from view behind the rim of the Valle del Bove (Fig. 7c, d). The horizontal component of movement of the white plume and dark density current was several tens of kilometers per hour. Within less than a minute from the initiation of these flows, a very large white plume soared skyward. The entire sequence of events was accompanied by no sound other than that produced by the ongoing Strombolian activity at the summit of the SEC, the clattering of falling rocks ejected from the emission points, and a few crackling noises resembling gunshots (possibly lightning).

Another significant explosive event producing ground-hugging vapor and ash clouds occurred at approximately

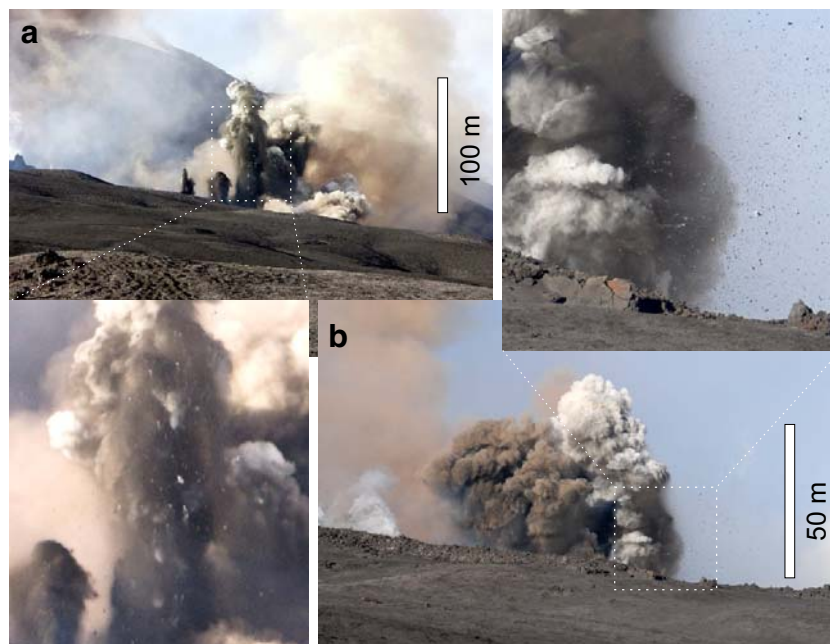


Fig. 6 The initial moments of the large explosive event at 1425 GMT, photographed at close range from S and SE. **a** Dark tephra jets and sideward-spreading vapor cloud (at right) emerging from the base of the Southeast Crater cone (seen partly in left background). Enlargement of main jet in 'a' shows how many of the ejected blocks were

followed by vapor trails. Photograph courtesy of Simone Genovese. **b** Initial tephra and vapor jet, presumably 1 or 2 s before **a** was taken. Most of the clasts seen airborne in the enlarged portion are followed by vapor trails. Photograph courtesy of Nino Mazzaglia



Fig. 7 Lateral propagation of the area of explosive tephra and vapor emission and development of highly mobile, ground-hugging vapor and ash clouds during <2 min after the first tephra and vapor jets (Fig. 6) at 1425 GMT on 16 November 2006. Note large reddish-brown ash plume descending through the breach created in the Southeast Crater cone's flank in **a**, showing a different hue than the more grayish tephra rising from the explosions at the cone's base. **b** Clearly shows the multiple

tephra and vapor jets rising from a number of spots. Ground-hugging white vapor plume is well ahead (spreading to the right) in **c**, but being surpassed by the much faster ash current in **d**. Time covered by this series of images is less than a minute. Photograph in **a** courtesy of Nino Mazzaglia, all other photos taken by Jane Applegarth, Lancaster University

1454 GMT. Like the event 30 min earlier, it started at some distance from the ESE base of the SEC cone with the uprise of a mixture of white steam and brown ash plumes from what appeared to be multiple sources. The details of the involved processes and extent of the flows are much less well documented than those of the 1425 events, but a mixed ash–vapor cloud once more spilled eastward and followed a similar path as did its predecessor.

Source area and deposits

Aerial and field studies of the source area and deposits of the largest 16 November PDCs were carried out during the 2 days after that event. These failed to reveal any evidence for the presence of an eruptive fissure in the area where the major explosions and flows originated. Instead, the area showed a complex morphology characterized by the remnants of the mobile block that had been extruded from the lower flank of the SEC cone and a complex assemblage of overlapping ash and coarse-grained blocky flow deposits and lava flows (Fig. 8). The remaining part of the extruded block was a blade-shaped crest, on both sides of which channels had been carved into the ground, and which were partly filled by coarse debris and lava flows (Fig. 8b). On

the adjacent SEC cone, a deep scar was incised into its SE flank where the new fracture had cut the slope.

The deposits produced by the 1425 GMT PDCs were emplaced to the E and ESE of the SEC and extended to a maximum distance of approximately 1.2 km (Fig. 4f). They consisted of a very thin (up to a few millimeters) extensive, lobate deposit (TM facies) of fine-grained lithic ash mantling the topography, and a thicker, coarse-grained heterolithic clastic deposit of much more limited extent (TC facies) whose transport and emplacement were strongly controlled by the morphology (Fig. 8). The southern and eastern margins of the TM deposit were clearly visible on aerial photographs taken shortly after emplacement, but its northeastern and northern margins were more diffuse due to wind-driven fallout from the dust plume and other airborne tephra and deposition on a complex morphology. The thicker coarse-grained flow (TC) partially eroded the base of the spatter cone at vent “B” and traveled several hundred meters beyond toward the Valle del Bove (Figs. 4f and 8a). Its levees and drained channeled morphology resembled that of thick ‘a’a flows emplaced in the same area—including the presence of prominent levees <3 m thick—but its overall color was brown due to the presence of abundant oxidized lithic material derived from the disintegrating flank of the SEC cone.

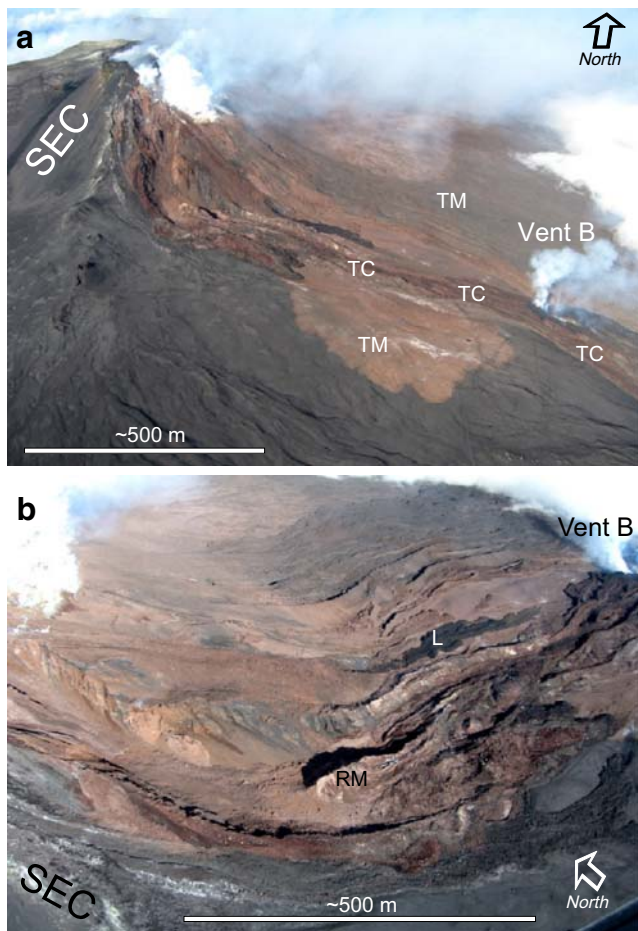


Fig. 8 Aerial views of the Southeast Crater (*SEC*), the huge collapse scar in its southeastern flank and the flow deposits of 16 November 2006, taken 1 day after the events. **a** The light-colored, lobate surge deposit (*TM*) is seen in the foreground and the morphologically controlled flow (*TC*) forming a dark streak links the ruptured flank of the Southeast Crater (at *left*) to the steaming vent “B” (see Fig. 1) at 2,800 m elevation (at *right*). **b** Source area of the explosive event of 1425 GMT on 16 November at the base of the Southeast Crater and *TC* deposit extending toward the steaming vent “B” (right background). Fin-shaped feature (*RM*) in lower center is a remnant of the portion of the flank of the Southeast Crater cone that had been pushed out of the flank and marks the approximate location of the major hydrovolcanic explosions at 1425 GMT. Note prominent channel morphology in the *TC* deposit and small, black tongue of lava (*L*) extruded late during the 16 November 2006 eruptive episode

Field observations confirmed that the *TM* deposit was pinkish in color and apparently contained few if any juvenile clasts (Fig. 9a), whereas the *TC* deposit contained variable amounts of deformed juvenile clasts that were still hot during emplacement (Fig. 9b). Cauliflower bombs were abundant in this deposit (Fig. 9b). Thermal images collected on 17 November revealed a maximum surface temperature of deposits in a channel adjacent to the vent “B” spatter cone of 187°C. This is significantly lower than the maximum temperature of 581°C at the base of the surface layer of clasts (at depths of 5–10 cm), which suggests that the surface deposits were underlain and heated

by still-hot lava buried by the debris flow. It is interesting to note that the early summit-fed lava flow of 16 November 2006 had taken exactly the same course (Fig. 4); this flow had been severed from its source by the enlargement of the collapse scar and ceased flowing before the major PDCs.

The deposit surrounded and partly buried a wooden, plastic-coated warning sign on a path at the southern margin of the deposit. This showed no evidence of heating (Fig. 9b) suggesting that at least some portions of the flow were cold at the time of emplacement. Most of the *TC* deposit was buried 3 days after emplacement under lava flows produced by the next eruptive episode from the *SEC* and by lavas erupted from vent “B.”

The 24 November 2006 event

The last documented occurrence of PDCs during the 2006 summit activity was recorded at 0817 GMT on 24

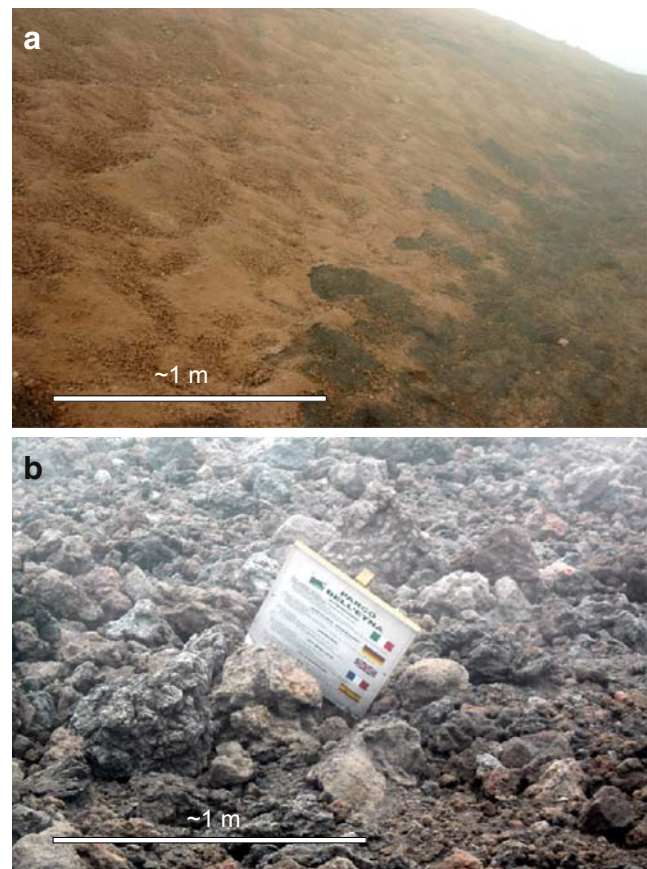


Fig. 9 **a** Facies *TM* emplaced by 16 November 2006 density current, consisting of a single thin layer of reddish-brown lithic ash, which is seen here covering older pyroclastics and footprints about 1 km SE of the Southeast Crater. **b** Field photograph of facies *TC* emplaced on 16 November 2006, showing a plastic-coated panel with tourist information entrained by the flow but showing no evidence of heating. Note the presence of breadcrust bombs (e.g., to the *left* of the panel). Photo taken 1 day after emplacement

November during a particularly explosive episode from the SEC. There were no trained observers to witness this event directly, but footage from the Schiena dell'Asino INGV-CT monitoring camera (approximately 5 km from the crater) and video-recorded by a tourist allowed a reconstruction of the main events. Vigorous eruptive activity (mostly ash emission with minor lava fountaining) had started from the summit vent of the SEC a few hours earlier, and lava had started to issue from a cluster of vents at the ESE base of the cone. At 0817:28, a dense, grayish-white plume suddenly appeared in the area of the effusive vents and shot downslope, followed instantaneously by a much larger and darker cloud that rapidly traveled toward the Valle del Bove rim and beyond. From the video footage, it is possible to establish that the toe of the advancing cloud moved approximately 1 km in 30 s, which corresponds to 120 km/h.

Intense explosive activity from the SEC continued throughout that day, causing heavy tephra fall over the area of the collapse and flows. This, coupled with deteriorating weather conditions during the following days, prevented investigations of the deposits. The area was buried under new lava flows during the next eruptive episode on 27 November.

Discussion

One of the outstanding features of the second (August–December) phase of the 2006 SEC eruptions is the repeated occurrence of a broad spectrum of PDCs and other mass-wasting processes. Many of these resulted from the gravitational collapse of portions of the SEC cone, and this was often exacerbated by eruptive activity, such as the passage of lava flows over outcrops of unstable rock. This category had some characteristics of debris falls as described by Branney and Kokelaar (2002, p. 28).

The early September events seem to have been caused mainly by the failure of unstable, strongly fractured and (at least locally) hydrothermally altered rocks which were bulldozed by advancing lava flows, for example when the upper and lower rims of the 2004–2005 collapse pit were breached by lava from the summit vent of the SEC and when lava subsequently flowed across the explosive vents of the July 2006 eruptive episode. However, nearly all of these events were accompanied by dense plumes of white vapor, which indicates that some interaction between the lava and water took place.

Many of the PDCs produced on 16 November consisted of basal avalanches overridden by rolling, ground-hugging, turbulent clouds of ash (phoenix clouds *sensu* Branney and Kokelaar 2002) mixed with varying quantities of water vapor, rising buoyantly. The flows described in this paper were highly mobile and traveled at speeds of several tens of kilometers per hour. In this sense, they were nearly identical

to “classic” pyroclastic flows, which commonly occur either during collapse of eruption columns or of lava domes, in most cases at silicic volcanoes.

Many basaltic phreatomagmatic eruptions produce pyroclastic density currents with some (e.g., La Palma in 1949; White and Schmincke 1999) producing dense flow-like currents and the more characteristic dilute “surges.” Other pyroclastic flows are known from particularly volatile-rich, explosive basaltic eruptions and have been described, amongst others, at Manam in Papua New Guinea (Taylor 1963) and Masaya in Nicaragua (Pérez and Freundt 2006; Wehrmann et al. 2006). For these eruptions, the pyroclastic flows were argued to form during the collapse of pyroclastic fountains or eruption columns. Similar, though smaller, currents were observed during some of the numerous episodes of fire-fountaining at the SEC on Etna in 2000; these were formed by the collapse of pyroclastic jets, especially when these were obliquely directed. In a very different scenario, pyroclastic flow-like density currents at Etna in October 1999 originated from gravitational collapse of a bulging and oversteepening accumulation of solid but still-hot lava (Calvari et al. 2002; Calvari and Pinkerton 2002; Behncke et al. 2003), similar to pyroclastic flows generated by the collapse of silicic lava domes like Unzen, Merapi, or Soufrière Hills.

The flows of 16 November were generated by yet another combination of processes, which need to be considered in more detail. We distinguish three main categories of PDCs: (a) rock falls and avalanches due to gravitational collapse of unstable portions of the SEC cone; (b) minor pyroclastic flow-like density currents at least partially induced by explosivity; and (c) major PDCs generated by hydromagmatic explosions.

Rock falls and avalanches due to gravitational collapse

Smaller flows, avalanches, and rockfalls, which entrained old and largely dry material from the crumbling portions of the cone, resulted mainly from gravitationally induced failure of unstable portions of the SEC cone. On 16 November, many of these mass flows were initiated from the head and lateral walls of the large scar opening in the southeast side of the cone. The main cause of collapse was undermining of the walls of the scar by flowing lava and failure of the headwall as lava poured from the summit area into the scar. Many of the collapse events within the scar produced reddish-brown plumes, distinct from the dark brown to black clouds of the explosively generated PDCs, and indicative of mostly older oxidized rock being involved.

Minor pyroclastic flow-like density currents partly induced by explosivity

The most common type of PDCs on 16 November occurred when lava flowed over or around unstable portions of the

SEC cone, leading to their failure and often interacting with moist rock incorporated in the ensuing mass flows. Gravity certainly played a significant role in powering this category of flows. These flows came rushing down the flanks of the cone, over a fall height of up to 250 m (the SEC cone is about 300 m tall on its eastern side), and in most cases, consisted of a dense cloud with a rounded or pointed nose, preceded at times by cascades of bouncing blocks (partly incandescent lava, partly old material derived from the cone) reminiscent of descriptions given for Montserrat and Unzen (Yamamoto et al. 1993; Branney and Kokelaar 2002). A variety of this category of flows is shown in Fig. 10.

Major pyroclastic density currents generated by hydromagmatic explosions

The large ground-hugging vapor and tephra clouds produced by the explosions at the base of the SEC cone at 1425 GMT of 16 November are an excellent example of decoupling of PDCs as described by Fisher (1995). They separated into (a) a dilute, vapor-cushioned, base surge-like current (TM) where clasts were presumably supported by fluid turbulence (Branney and Kokelaar 2002), and (b) an areally more restricted basal avalanche (TC). The relatively high viscosity and yield strength of the latter were documented by the marked lateral levees of the deposit and the erosive force exerted on the spatter cone at vent

“B.” The TM deposit was emplaced as a laminar sheet, consisting of a single unit where examined (that is, in the distal areas of the deposit), although a more complex internal stratigraphy may have occurred in its proximal portions. In contrast, the TC avalanche laid down a chaotic, heterolithologic deposit. Both deposits were emplaced in a single pulse—the explosive activity at 1425 GMT lasted only a few tens of seconds—and thus each consists of a single flow unit. Whatever material may have been added by PDCs produced by the 1454 GMT explosion is inconspicuous and/or indistinguishable from the 1425 GMT material (Fig. 11).

In contrast with the smaller, largely gravity-driven flows described in the previous section, the 1425 GMT flows originated in a relatively flat area, which was not subject to gravitational failure even under large stresses. However, in common with many of the smaller PDCs, the initiation of the 1425 GMT flows was characterized by conspicuous explosive activity. The “boiling” action seen at the base of the rolling clouds of the minor flows indicates explosive fragmentation occurring along, and even within, the descending basal avalanches. Likewise, rising and collapsing tephra jets occurred over an increasing area along with the expansion of the ground-hugging clouds of the 1425 GMT flows, only on a much larger scale. We have failed to recognize similar phenomena in descriptions and video footage of pyroclastic flows moving on land, but apparently such explosions are common at the base of pyroclastic

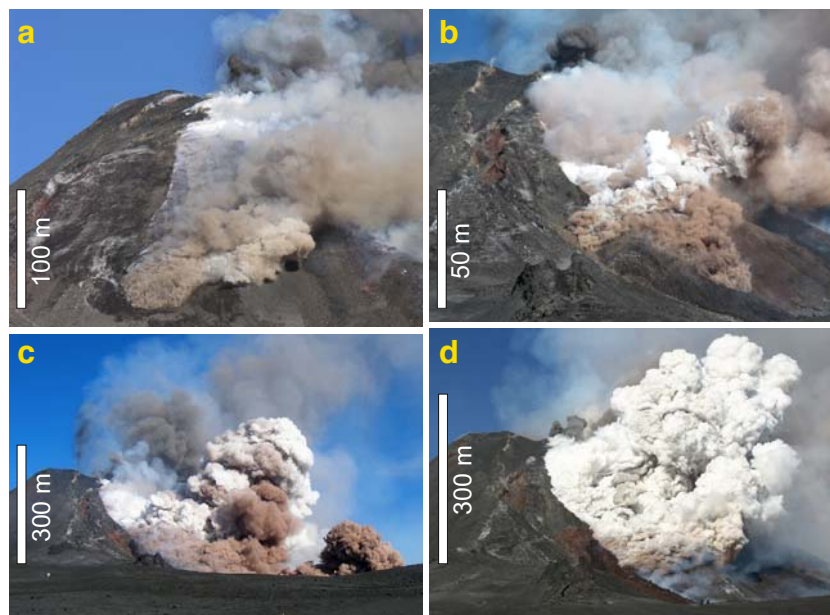
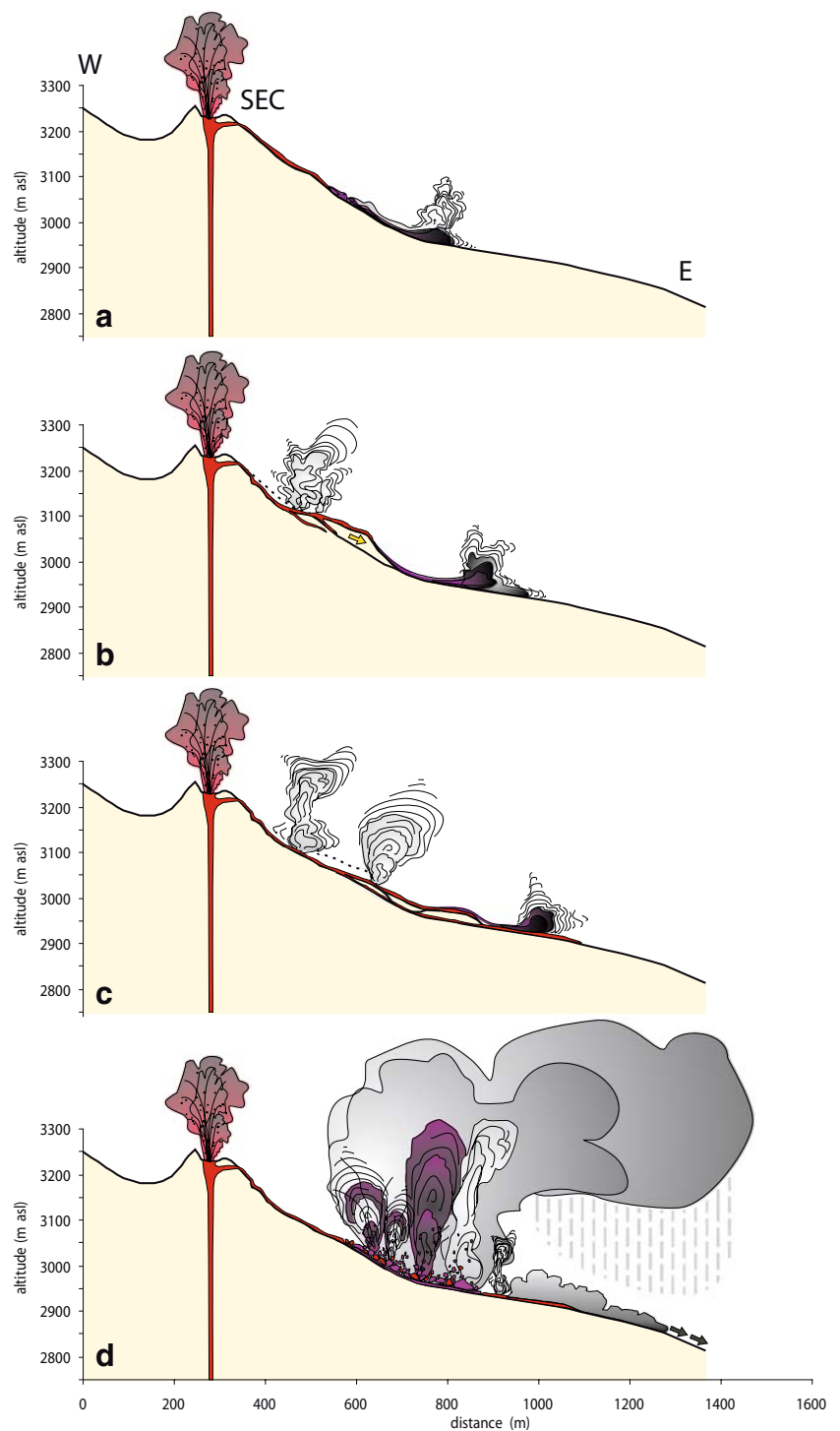


Fig. 10 Various aspects of typical small- to modest-sized pyroclastic density currents on the forenoon of 16 November 2006. **a** Small flow resulting from mixing of hot lava and moist rocks that descends from the lower termination of the opening crack on the southeast flank of the Southeast Crater at 0714 GMT (photo courtesy of Nino Mazzaglia). **b** Bifurcating small flow issues from the lower end of

the large scar that has developed from the original crack, 0938 GMT. Note abundant vapor at the origin of the flow. **c** Modest-sized flow extending a few hundred meters beyond the base of the Southeast Crater cone and dense vapor plume billowing from the growing scar in the side of the cone, 0901 GMT. Note reddish hue of the ash cloud. **d** Vapor-rich flow issuing from the lower end of the scar at 1147 GMT

Fig. 11 Interpretative east–west section through the Southeast Crater cone, showing the erosion of an active lava flow into the flank and formation of the large scar (**a, b**), detachment and downslope movement of a block from the lower flank (**b, c**), and origin of pyroclastic density currents on 16 November 2006. **d** Shows the site and superficial nature of the large hydromagmatic explosions at 1425 GMT at the base of the cone



flows advancing over water (Hart et al. 2004; Edmonds and Herd 2005). Our interpretation of these events envisages rapid heating of water in the moist rock fragments detached from the disintegrating cone. The superheated water caused further fragmentation of lithics, exposure of fresh water-saturated surfaces, and a runaway fragmentation process rapidly developed. Such a mechanism may have been facilitated in an environment of poorly interconnected pores

within lithic clasts, leading to decompression upon breakage of clasts and thus new explosive bursts. This was enhanced by continuing fragmentation and remingling of moist old rock and hot lava clasts as they were transported away with the PDCs to even greater distances from the site of the first explosions.

What distinguishes the PDCs of 1425 GMT from “classic” pyroclastic flows is the mechanism that generated

them, which was not related to explosive activity at an eruptive vent or to the collapse of a growing lava dome, and their significantly lower temperatures at least in places, as indicated by the tourist sign entrapped but not damaged by the TC flow (Fig. 9b). This mechanism needs to be seen in the light of the evolution of events during the hours preceding the major explosion and flows.

What caused the major pyroclastic density currents of 16 November 2006?

One of the questions arising from our observations on 16 November was whether the major PDCs at 1425 GMT were generated by the opening of new eruptive vents along a radially propagating fissure or whether there was a superficial mechanism.

The opening of new fractures on the flanks of the SEC cone has been observed on numerous occasions in the past (Behncke et al. 2006) and also occurred on several occasions during the weeks before and after the 16 November events. Typically, such fractures propagate downslope in a matter of a few minutes, often with lava fountaining from numerous vents along the fracture, and culminating with major fountains and/or lava flow emission from the lowest vents. Activity at the summit of the SEC and from the early formed, upper portions of the fracture commonly ends rapidly after full development of the fracture.

There are a number of arguments that indicate that the cause of the 1425 GMT PDCs was not related to the injection of a dike from depth. (1) Ground and aerial observations carried out after 16 November failed to reveal a fissure in the area where the explosions and major PDCs originated. (2) The opening of an eruptive fissure would have been marked by lava emission and fountaining, as during virtually all flank and subterminal eruptions from Etna. (3) After the explosive events of 1425 and 1454 GMT, no further activity occurred from the hypothetical fissure, whereas explosive and effusive activity continued at the summit of the SEC for several hours. (4) Eruption-related seismicity, such as tremor amplitude and explosion quakes showed a marked *drop* about 30 min *before* the 1425 GMT event (S. Falsaperla, personal communication 2007). All these facts contrast markedly with what is known from multiple observations of flank eruptive fissures opening on Etna (Calvari et al. 1994b; Bertagnini et al. 1990; Calvari and INGV staff 2001; Acocella and Neri 2003; Behncke and Neri 2003; Neri et al. 2004, 2005; Andronico et al. 2005).

The processes leading to the culminating events on the early afternoon of 16 November started with the advance of lava fed by the summit vents through the strongly fractured and hydrothermally altered southeast slope of the cone. A

plausible explanation is that the lava intruded in a sill-like manner between strata making up the SEC cone. Because the strata show an outward inclination more or less at the angle of the outer slope of the cone, this intrusion was assisted by gravity. Intrusion along this interface and the subsequent failure of this part of SEC were facilitated by a potential plane of weakness at the contact between the weaker older rocks making up the cone and the slope of the new pyroclastic cone that had largely filled the 2004–2005 collapse pit since September 2006. When passing from the newly accumulated material toward the older, unstable material, lava could easily intrude at the boundary between these materials and cause its failure. The magmatic sill would create a low strength layer at the base of the block and this would facilitate its movement downslope. A similar process involving the intrusion of lava along a major discontinuity was inferred to initiate the instability of the northwestern wall of the Bocca Nuova in October 1999 by Calvari and Pinkerton (2002) who also presented evidence of pervasive penetration of lava through the SEC in the same period (Calvari et al. 2002).

The lava eroded a path through the highly unstable and weakened material, opening a deep scar into the upper portion of the SEC cone. The later stages of the opening of this erosion scar were accompanied by the slow structural extrusion and piecemeal disintegration of a large slump block of the lower flank of the SEC cone (Figs. 5 and 11b). We suggest that the combined effect of the pressure exerted by the lava at the headwall of the block, coupled with high magmatic pressures beneath the block and marginal shear stresses of lava in channels on either side of the block, led to the peculiar structural extrusion and fracturing of this block. The lava also intruded into cracks within the block, further enhancing its destabilization and disintegration and permitting the lava to interact with the water-soaked interior of the block.

Still photography and video footage reveal that, shortly before the major explosive event at 1425 GMT, the block had flattened out noticeably and advanced well beyond the cone's base (Figs. 5, 1345 frame, and 11c) to the area where the explosions were to take place. At this time, the remainder of the extruding block was rapidly moving forward, as could be seen from the constant crumbling of its margins, especially at the front. Some of the material involved was incandescent, evidence that in some places fresh lava (fed from the SEC summit vents) had broken through the disintegrating block and was mingling with various quantities of water-soaked rock constituting the block. It was specifically within this block that the first fountains of ash and blocks appeared 1 min before the culminating events.

It has furthermore to be noted, that during its later stages of advance, the structurally extruding block covered hot,

partly still-moving lavas emplaced during the preceding surges of lava emission from the lower end of the opening fracture. This, together with the lava intruding into and flowing above the moist material, must have created ideal conditions for some of the moist rock to be enclosed by hot lava, causing explosive magma–water interaction similar to processes observed when lava enters, and mingles with, water or wet sediments in fuel–coolant or fuel–impure coolant interactions (e.g., Wohletz 1986; White 2006; Mattox and Mangan 1997; Zimanowski and Büttner 2002; Martin and Németh 2007; Németh and Martin 2007). The absence of any conspicuous sound during the main explosive sequence of 1425 GMT might be taken as evidence against a typical fuel–coolant interaction, although sound may have been muffled by the peculiar physical properties of the large quantities of water-saturated altered rock involved.

The main explosive sequence was characterized by the uprise of cypressoid jets of dark brown tephra mixed with water vapor, typical of hydromagmatic activity. Photographs taken during the first moments of that activity show that many ejected blocks were followed by vapor trails (Fig. 6), suggesting that they were derived from the interaction of the moist older rock with active lava. This coincides well with the ubiquitous presence of strongly altered rock fragments in the TC deposit (Fig. 9b).

Our conclusion from these observations is that the major explosions and PDCs at 1425 GMT on 16 November 2006 were caused entirely by magma–water interaction as magma intruded into the block extruded from the lower flank of the SEC cone, which was constituted by water-soaked, hydrothermally altered rock.

Role of hydrothermal fluids

A primary role in the trigger mechanisms of the 16 November events was certainly played by hydrothermal fluids percolating through the structure of the SEC cone, as highlighted by the evident reddish-brown color of the light fraction of the collapsing materials due to intense mineral alteration (TM deposit, Fig. 9a). The importance of hydrothermally altered volcanic rocks in promoting sector collapse at more explosive volcanoes than Etna has been recognized, evaluated, and modeled in recent years (Lopez and Williams 1993; Reid et al. 2001).

Hydrothermal systems are almost ubiquitous features on active volcanoes. The scale of these systems is highly variable, ranging from large-sized voluminous hydrothermal reservoirs that affect most of the volcano structure to small-sized local thermal pockets close to the main active vents (e.g., Hochstein and Browne 2000). The small-sized local thermal pockets close to the main active vents seem to be the type present at Etna where hydrothermal reservoirs of significant extension are unlikely, and only relatively

small reservoirs have been hypothesized within the deeper levels of the volcano edifice, based on the geochemical features of local groundwaters (Giammanco et al. 1998a; Brusca et al. 2001). Much smaller hydrothermal systems on Etna, whose surface evidence is the presence of fumarole fields and steamy grounds, have been reported close to Etna's summit craters since the early twentieth century (Ponte 1927; Aubert et al. 1984; Aubert and Baubron 1988; Aubert 1999; Giammanco et al. 1998b, 1999; Alparone et al. 2004). These systems depend upon the existence of high-permeability zones corresponding to relatively shallow fractures and faults in the topmost part of the volcano. Even close to the rims of the summit craters, fumaroles and steam vents are distributed almost exclusively along fractures, mostly formed by the structural instability of the crater rims themselves. However, the seemingly rare occurrence of events such as those of 16 November may be explained by the fortuitous combination of several concurrent factors like steepness of the cone, its intense fracturing, and presence of widespread hydrothermal activity, the latter probably having increased dramatically after the end of the almost persistent volcanic activity at the SEC in July 2001.

Prolonged (about 4 years) absence of magma within the uppermost part of SEC feeder conduit allowed partial cooling of its cone starting from its outer portions, thus promoting free circulation of hydrothermal fluids into its volcanic rock layers, and enough time subsequently for the chemical alteration of the volcanic materials. The SEC hydrothermal system may have developed thanks to a combined action of condensation of high-enthalpy acid magmatic fluids that rise from depth along the almost closed, but still permeable, SEC conduit and downward percolation of cold meteoric water from the outer surface of the cone into its deeper strata.

An attempt can be made to assess the likelihood that hydrothermal fluids can alter and mechanically modify the volume of rock making up the portion of the SEC cone that collapsed on 16 November 2006. Unfortunately, direct measurements of the amount and type of altered rock at the SEC are not available because the collapsed material was buried soon after its emplacement by newer eruptive products and access to the scar left by the collapse in the flank of the SEC was too hazardous. However, aerial and field observations of the PDC deposits (see, e.g., Figs. 8 and 9) revealed that a significant proportion was strongly altered (attested to by its widespread brownish color). In general, interaction between acid-sulfate solutions, produced by the absorption and oxidation of H₂S-bearing vapors in shallow groundwaters, and rocks determines the formation of kaolinite, alunite, gypsum, opal, and hydrated iron oxides (Steiner 1977). This mineral assemblage is typical of steam-heated zones close to the surface, as is the case of the SEC hydrothermal system. A recent geochem-

ical study of weathering of Etna's rocks by groundwaters circulating in its edifice (Aiuppa et al. 2000) led to an estimated chemical erosion rate of about 2.3×10^5 t/a and a specific erosion rate of 200 t/km²/a, considering a total volcanic surface of 1,150 km². This figure is higher than the average global rate for chemical erosion at the Earth's surface (26 t/km²/a, Berner and Berner 1996), indicating the high intensity of rock leaching in volcanic environments. The alteration minerals produced by basalt weathering at Etna are primarily clays, mostly smectites and kaolinite, but also oxyhydroxides (Aiuppa et al. 2000; Giammanco et al. 2007). In any case, all of the above-mentioned altered materials have low mechanical strength. To assess the extent of rock alteration at the SEC, we need to estimate the volume of collapsed rock and the volume of fluids required to chemically alter it. A simple calculation of the volume of the collapsed sector can be performed assuming that the SEC cone is a regular cone having a radius of 350 m (i.e., the distance from the central axis of the SEC cone to its perimeter) and a height of 250 m (height of the SEC calculated considering its base set at an altitude of 2,950 m asl) and that the opening angle of the collapsed sector is about 22.5°, that is to say that the volume of this sector corresponds, roughly, to one-sixteenth of the volume of a cone. The obtained sector volume is about 2.0×10^6 m³. This volume is a significant overestimate because the collapse did not affect the whole sector of the SEC cone down to the core of its structure, and part of the collapsed flank was structurally extruded without being dismantled. Another way to calculate the collapsed volume is to measure the surface covered by the TC flow (i.e., about 73,000 m²) and multiply it by its average thickness. Direct measurements of the flow thickness were not performed, yet a reasonable estimate is to assume an average thickness of 3 m. In this way, we obtain a volume of roughly 220,000 m³ for the TC flow, an order of magnitude lower than the volume obtained for the cone sector. This is considered to be a more reasonable estimate of the volume of altered rock. For a rock density of 2,500 kg/m³, the mass of the collapsed sector having formed the TC flow is approximately 550,000 t.

Many different factors, such as rock mineralogy, fluid geochemistry, temperature, and saturation conditions of hydrothermal fluids, determine the rates of rock alteration. No such data are available for the SEC hydrothermal system, so our assumptions have to be based on data from other volcanoes. Lopez and Williams (1993) calculated that the ratio between the weight of reacting fluids passing through the hydrothermal system of Nevado del Ruiz and the weight of hydrothermally altered volcanic rock was about 100/1. This ratio gave an amount of altered rock of 12,600 m³ of rock per year. In much smaller systems, like Poás, the altered rock was calculated to be 1,650 m³ per

year (Rowe et al. 1992). Assuming that the SEC is altered at a similar rate to Nevado del Ruiz, the mass of fluid required to alter the mass of rock corresponding to the TC flow is in the order of 5.5×10^7 t. However, this is unrealistically high because not the entire mass of the TC flow was hydrothermally altered. If we assume a maximum of 30 wt% of alteration minerals within the TC flow, following the results in Lopez and Williams (1993), then up to 10,000 t/day of water are required to flow through the volume of rock that mobilized on 16 November 2006. This is based on our estimate of 5 years of alteration, during the period of eruptive quiescence of the SEC before its reactivation in 2006. The annual rainfall in the summit area of Etna of approximately 500 mm (Cosentino 1974) corresponds to about 40 t/day of rain over the area of the collapsed sector (about 30,000 m²). Although no data are available about the amount of snow fall, this will be insignificant compared with the volume of water required for alteration. This suggests that the greatest contribution to the hydrothermal system of SEC is magmatic.

An estimate of the water vapor release from Etna's summit craters can be obtained using the data provided by Aiuppa et al. (2007) based on recent measurements of the CO₂/SO₂ and CO₂/H₂O ratios. During 2006, the CO₂/SO₂ ratio in Etna's crater plume varied between 0.5 and 25 and the CO₂/H₂O ratio over this period varied between 0.01 and 0.5, resulting in an H₂O/SO₂ ratio of 50 at both extremes. Based on crater emission measurements on Etna's craters by Salerno et al. (2005), the average SO₂ flux during the intereruptive period July 2001 to the start of the 2002–2003 eruptions (471 days) was approximately 950 t/day. During the 2002–2003 eruption (85 days), this rose to approximately 9,900 t/day, and between the end of the 2002–2003 eruption and early 2005, it was about 1,900 t/day. Assuming the latter value to be characteristic of the intereruptive period before the onset of the July 2006 eruption (1,269 days), we multiplied each average flux value for the corresponding number of days, summed the results, and then divided by the total number of days from July 2001 to July 2006 (i.e., 1,825). The calculated SO₂ flux is approximately 2,000 t/day, from which it can be shown that, on average, during this period, approximately 100,000 t/day of water was released through the four summit craters of Etna. It is interesting to note that Burton et al. (2006), using a similar approach, calculated a water flux of 380,000 t/day from the SEC on 23 October 2006. Furthermore, for several months before 16 November 2006, fumarolic activity was much stronger than usual in the area where the large fracture later opened; often giving rise to a dense plume that hid much of that side of the cone. Notwithstanding the high variability of the crater water flux from the SEC, it is more than sufficient to have caused the high degree of alteration to rocks in the S flank of SEC.

Another factor that may have contributed to alteration, during the weeks before the 16 November event, was an increase in permeability of the SEC cone by extensive fracturing as more and more vents became active on its flanks and near its base. This fracturing may have also led to a dramatic increase in the contact surface area between hot magmatic/hydrothermal fluids and fluid-soaked rocks comprising the cone when lava flowed over, or intruded into, the moist rocks.

Hazards

The collapse events and PDCs observed during the 2006 SEC eruptions serve as a vivid reminder that, although only moderately explosive eruptions take place on Etna, it is capable of producing highly hazardous activity on a local scale. Unexpected phreatic explosions at the summit (Murray 1980) are only one of the hazards confronting those who visit the summit region of Etna. During the past few decades, PDCs have occurred at Etna's summit repeatedly (Calvari and Pinkerton 2002; Behncke et al. 2003), although the mechanisms generating them have varied strongly and were, in a number of cases, due to unique combinations of factors, each of which alone would not have generated any unusual phenomena.

In our interpretation, the combination of factors that produced density currents at the Bocca Nuova in 1999 (see the “Introduction” section; Calvari and Pinkerton 2002; Behncke et al. 2003) were exceptional and are not likely to be repeated in the short-term. The SEC remains unstable, however, and may still contain a significant proportion of weak, hydrothermally altered rocks that might facilitate a repetition of events like those of 16 November 2006, especially in the light of renewed eruptive activity in 2007. In addition, fountain-collapse pyroclastic flows like those in 2000 have occurred repeatedly and they may be expected any time if one of the summit craters goes through a period of episodic fire-fountaining. Most importantly, though, there are clearly many ways in which different factors combine to produce hazardous pyroclastic density currents at Etna.

Runout lengths of PDCs described above were in the range of 1–1.5 km, thus representing no threat to populated areas or tourist infrastructures located on the slopes of the volcano. We are confident that events like those of 16 November 2006 are encountered only in the summit region. Consequently, the only source areas of hazardous PDCs are close to the summit, and the threat posed by such events is primarily to visitors of that area. PDCs such as those of 16 and 24 November 2006 may not have attained the temperatures of many pyroclastic flows, but are considered hot enough to be deadly, especially because of their high steam content. Moreover, their high speed would have subjected

any living being to extremely high and possibly lethal dynamic pressure (sensu Baxter et al. 1998; Spence et al. 2007). Death or serious injury would have furthermore resulted from the impact of rock fragments carried with the currents, at least in the dense, topography-controlled portion of the 16 November PDCs, whereas survival might have been possible in the more dilute portion of the flow that led to the deposition of the thin TM deposit.

Based on these assumptions, all areas within about 1.5 km from each of the four summit craters should be considered potentially hazardous during strong summit eruptions that might result in the formation of pyroclastic density currents.

Conclusions

The 2006 summit (Southeast Crater) eruptions of Etna were, in most senses, a repetition of previous eruptions at this volcano. At times, however, they were accompanied by a variety of minor and larger collapse events that triggered rockfalls and small pyroclastic density currents and by hydromagmatic explosions that resulted in larger and highly mobile PDCs. Many of the smaller events occurred when lava flowed over unstable portions of the SEC cone and triggered their failure. Such unstable areas had become increasingly extensive during the years previous to the 2006 eruptions, most notably during the formation of a pit crater on the cone's east flank in 2004–2005.

The largest hydromagmatic events and related PDCs of this period occurred on 16 November during an otherwise quite “normal” episode of Strombolian activity and lava effusion from the SEC. The explosions were rootless because they occurred in locations away from eruptive vents and were the result of the mixing and interaction of hot lava and fluid-soaked rocks derived from the southeastern flank of the SEC cone.

Failure of the flank was facilitated by the presence of considerable volumes of weak, hydrothermally altered rock, after several years of intense fumarolic activity in this sector of the cone. Lava erupted from the summit vents of the SEC could thus easily erode and intrude into this unstable material, leading to the detachment and mobilization of a large block of the cone's lower flank. The material constituting this block became increasingly incorporated and mixed with hot lava, and contact explosions became more violent, culminating at 1425 GMT. The PDCs produced by the major explosions contained a minor quantity of fresh lava and abundant altered material, reflecting the approximate proportions of material involved in the hydromagmatic activity.

The main conclusion of our observations and analysis of the 16 November 2006 events is that potentially hazardous

volcanic density currents similar to pyroclastic flows can be generated away from erupting vents during mildly explosive basaltic eruptions by interaction of hot lava with moist, hydrothermally altered rock.

These observations may have implications for other volcanoes where lava flows (independently of their composition) move over, or intrude into, fluid-soaked, hydrothermally altered and strongly fractured rocks. Both catastrophic collapse and fast-moving PDCs can be expected to occur, even during predominantly effusive eruptions at large stratovolcanoes without involving any of the classic mechanisms of pyroclastic flows or volcanic debris avalanches.

Acknowledgements A part of this research was funded by the Istituto Nazionale di Geofisica e Vulcanologia (INGV) and by the Dipartimento per la Protezione Civile (Italy). We thank our colleagues at the INGV-CT, in particular Mike Burton and Giuseppe Salerno who provided the observations, photographs, and video footage of different phases of the events described in this paper; Giovanni Tomarchio of the Italian RAI television network, for letting us view his original video footage of the 16 November 2006 activity and pyroclastic density currents; Simone Genovese for providing still photographs and video footage of the same events; Nino Mazzaglia for sharing his unique and impressive photographic collection of the 2006 summit eruptions; Jane Applegarth for her photographs of the 16 November activity; and the helicopter pilots of the National Civil Defense Agency for flying us safely over the volcano during many crucial stages of the 2006 activity. Ken Wohletz is acknowledged for the very helpful thoughts and comments on an early version of the manuscript. The very inspiring and stimulating reviews by Greg Valentine and James White helped to bring out more strongly the essence of this paper.

References

- Acocella V, Neri M (2003) What makes flank eruptions? The 2001 Etna eruption and its possible triggering mechanism. *Bull Volcanol* 65:517–529, DOI [10.1007/s00445-003-0280-3](https://doi.org/10.1007/s00445-003-0280-3)
- Aiuppa A, Allard P, D'Alessandro W, Michel A, Parello F, Treuil M, Valenza M (2000) Mobility and fluxes of major, minor and trace metals during basalt weathering and groundwater transport at Mt. Etna volcano (Sicily). *Geochim Cosmochim Acta* 64:1827–1841
- Aiuppa A, Federico C, Giudice G, Gurrieri S, Liuzzo M, Moretti R, Shinohara H, Valenza M (2007) Real-time detection of volcanic plume H₂O, CO₂ and SO₂ as a precursor to 2006 Mt. Etna eruptions. *Geophys Res Abstr* 9:01863
- Alparone S, Andronico D, Giammanco S, Lodato L (2004) A multidisciplinary approach to detect active pathways for magma migration and eruption in a basaltic volcano: the upper southern flank of Mt. Etna (Sicily, Italy) before the 2001 eruption. *J Volcanol Geotherm Res* 136:121–140, DOI [10.1016/j.jvolgeores.2004.05.014](https://doi.org/10.1016/j.jvolgeores.2004.05.014)
- Andronico D, Branca S, Calvari S, Burton MR, Caltabiano T, Corsaro RA, Del Carlo P, Garfi G, Lodato L, Miraglia L, Murè F, Neri M, Pecora E, Pompilio M, Salerno G, Spampinato L (2005) A multidisciplinary study of the 2002–03 Etna eruption: insights for into a complex plumbing system. *Bull Volcanol* 67:314–330, DOI [10.1007/s00445-004-0372-8](https://doi.org/10.1007/s00445-004-0372-8)
- Aubert M (1999) Practical evaluation of steady heat discharge from dormant active volcanoes: case study of Vulcarolo fissure (Mount Etna, Italy). *J Volcanol Geotherm Res* 92:413–429, DOI [10.1016/S0377-0273\(99\)00088-8](https://doi.org/10.1016/S0377-0273(99)00088-8)
- Aubert M, Baubron JC (1988) Identification of a hidden thermal fissure in volcanic terrain, using a combination of hydrothermal convection indicators and soil-atmosphere analysis. *J Volcanol Geotherm Res* 35:217–225, DOI [10.1016/0377-0273\(88\)90018-2](https://doi.org/10.1016/0377-0273(88)90018-2)
- Aubert M, Auby R, Bourlet Y, Bourlet F (1984) Contribution à la surveillance de l'activité de l'Etna à partir de l'étude des zones fumerolliennes. *Bull Volcanol* 47:1039–1050, DOI [10.1007/BF01952359](https://doi.org/10.1007/BF01952359)
- Baxter PJ, Neri A, Todesco M (1998) Physical modelling and human survival in pyroclastic flows. *Nat Hazards* 17:163–176, DOI [10.1023/A:1008031004183](https://doi.org/10.1023/A:1008031004183)
- Behncke B, Neri M (2003) The July–August 2001 eruption of Mt. Etna (Sicily). *Bull Volcanol* 65:461–476, DOI [10.1007/s00445-003-0274-1](https://doi.org/10.1007/s00445-003-0274-1)
- Behncke B, Neri M, Carniel R (2003) An exceptional case of endogenous lava dome growth spawning pyroclastic avalanches: the 1999 Bocca Nuova eruption of Mt. Etna (Italy). *J Volcanol Geotherm Res* 24:115–128, DOI [10.1016/S0377-0273\(03\)00072-6](https://doi.org/10.1016/S0377-0273(03)00072-6)
- Behncke B, Neri M, Nagay (2005) Lava flow hazard at Mount Etna (Italy): new data from a GIS-based study. In: Manga M, Ventura G (eds) Kinematics and dynamics of lava flows. *Geological Society of America Special Paper* 396:189–209, DOI [10.1130/2005.2396\(13\)](https://doi.org/10.1130/2005.2396(13))
- Behncke B, Neri M, Pecora E, Zanon V (2006) The exceptional activity and growth of the Southeast Crater, Mount Etna (Italy), between 1996 and 2001. *Bull Volcanol* 69:149–173, DOI [10.1007/s00445-006-0061-x](https://doi.org/10.1007/s00445-006-0061-x)
- Berner EK, Berner RA (1996) *Global environment: water, air, and geochemical cycles*. Prentice-Hall, New Jersey
- Bertagnini A, Calvari S, Coltelli M, Landi P, Pompilio M, Scribano V (1990) The 1989 eruptive sequence. In: Barberi F, Bertagnini A, Landi P (eds) Mt. Etna: the 1989 eruption. CNR-GNV Giardini, Pisa, pp 10–22
- Brand BD, White CM (2004) Base-surge mechanisms and structures, an example from Sinker Hole, ID, Western Snake River Plain. *Geol Soc Am Abstr Prog* 36(4):84
- Branney MJ, Kokelaar P (2002) Pyroclastic density currents and the sedimentation of ignimbrites. *Geol Soc London Mem* 27:1–143
- Brusca L, Aiuppa A, D'Alessandro W, Parello F, Allard P, Michel A (2001) Geochemical mapping of magmatic gas–water–rock interactions in the aquifer of Mount Etna volcano. *J Volcanol Geotherm Res* 108:199–218, DOI [10.1016/S0377-0273\(00\)00286-9](https://doi.org/10.1016/S0377-0273(00)00286-9)
- Burton MR, Neri M, Andronico D, Branca S, Caltabiano T, Calvari S, Cosaro RA, Del Carlo P, Lanzafame G, Lodato L, Miraglia L, Salerno G, Spampinato L (2005) Etna 2004–2005: an archetype for geodynamically-controlled effusive eruptions. *Geophys Res Lett* 32:L09303, DOI [10.1029/2005GL022527](https://doi.org/10.1029/2005GL022527)
- Burton M, Caltabiano T, Bruno N, La Spina A, Longo V, Murè F, Randazzo D, Salerno G (2006) Aggiornamento eruzione al 27 Ottobre 2006: composizione e flusso di gas emesso dell'Etna. INGV-CT report UFGV2006/125:1–4
- Calvari S, the INGV–Sezione di Catania scientific staff (2001) Multidisciplinary approach yields insight into Mt. Etna 2001 eruption. *EOS Trans Am Geophys Union* 82:653–656
- Calvari S, Behncke B (2006) Etna: lava flows from multiple vents during 22 September to 4 November. *Bull Glob Volcanism Netw* 31(10):2–3
- Calvari S, Behncke B (2007) Etna: episodes of eruptions continue between 4 November and 14 December 2006. *Bull Glob Volcanism Netw* 32(2):22–26
- Calvari S, Pinkerton H (2002) Instabilities in the summit region of Mount Etna during the 1999 eruption. *Bull Volcanol* 63:526–535, DOI [10.1007/s004450100171](https://doi.org/10.1007/s004450100171)

- Calvari S, Coltelli M, Müller W, Pompilio M, Scribano V (1994a) Eruptive history of South-Eastern crater of Mount Etna, from 1971 to 1994. *Acta Vulcanol* 5:11–14
- Calvari S, Coltelli M, Neri M, Pompilio M, Scribano V (1994b) The 1991–93 Etna eruption: chronology and lava flow field evolution. *Acta Vulcanol* 4:1–14
- Calvari S, Neri M, Pinkerton H (2002) Effusion rate estimations during the 1999 summit eruption on Mt. Etna, and growth of two distinct lava flow fields. *J Volcanol Geotherm Res* 119:107–123
- Calvari S, Lodato L, Neri M, Behncke B, Norini G, Consoli O (2006) Changes in morphology of SE Crater and the emission of lava flows to the SSE. *Bull Glob Volcanism Netw* 31(8):2–3
- Chester DK, Duncan AM, Guest JE, Kilburn CRJ (1985) Mount Etna. The anatomy of a volcano. Chapman and Hall, London
- Coltelli M, Del Carlo P, Vezzoli L (1998) Discovery of a Plinian basaltic eruption of Roman age at Etna volcano, Italy. *Geology* 26:1095–1098, DOI [10.1130/0091-7613\(1998\)026<1095:DOAPBE>2.3.CO;2](https://doi.org/10.1130/0091-7613(1998)026<1095:DOAPBE>2.3.CO;2)
- Corsaro RA, Cristofolini R, Patané L (1996) The 1669 eruption at Mount Etna: chronology, petrology and geochemistry, with inferences on the magma sources and ascent mechanisms. *Bull Volcanol* 58:348–358, DOI [10.1007/s004450050144](https://doi.org/10.1007/s004450050144)
- Cosentino M (1974) Il regime pluviometrico sull' Etna negli anni 1921–1971. *Atti Acc Gioenia Sci Nat* 6:37–52
- Crisci GM, Di Gregorio S, Rongo R, Scarpelli M, Spataro W, Calvari S (2003) Revisiting the 1669 Etnean eruptive crisis using a cellular automata model and implications for volcanic hazards in the Catania area. *J Volcanol Geotherm Res* 123:211–230, DOI [10.1016/S0377-0273\(03\)00037-4](https://doi.org/10.1016/S0377-0273(03)00037-4)
- CVGHM (Centre of Volcanology and Geological Hazard Mitigation) (2006) Merapi: mid-2006 brings multiple pyroclastic flows that kill two, and travel up to 7 km. *Bull Glob Volcanism Netw* 31(5):10–11
- De Rita D, Frazzetta G, Romano R (1991) The Biancavilla–Montalto ignimbrite (Etna, Sicily). *Bull Volcanol* 53:121–131, DOI [10.1007/BF00265417](https://doi.org/10.1007/BF00265417)
- Druitt TH (1998) Pyroclastic density currents. In: Gilbert JS, Sparks RSJ (eds) The physics of explosive volcanic eruptions. *Geol Soc London Spec Pub* 145:145–182, DOI [10.1144/GSL.SP.1996.145.01.08](https://doi.org/10.1144/GSL.SP.1996.145.01.08)
- Duncan AM, Dikken C, Chester DK, Guest JE (1996) The 1928 eruption of Mount Etna volcano, Sicily, and the destruction of the town of Mascali. *Disasters* 20:1–20
- Edmonds M, Herd RA (2005) Inland-directed base surge generated by the explosive interaction of pyroclastic flows and seawater at Soufrière Hills volcano, Montserrat. *Geology* 33:245–248, DOI [10.1130/G21166.1](https://doi.org/10.1130/G21166.1)
- Fisher RV (1995) Decoupling of pyroclastic currents: hazards assessments. *J Volcanol Geotherm Res* 66:257–263, DOI [10.1016/0377-0273\(94\)00075-R](https://doi.org/10.1016/0377-0273(94)00075-R)
- Freundt A, Wilson CJN, Carey SN (2000) Ignimbrites and block-and-ash flow deposits. In: Sigurdsson H, Houghton BF, McNutt SR, Rymer H, Stix J (eds) *Encyclopedia of volcanoes*. Academic, San Diego, pp 581–599
- Gemmellaro C (1843) Sulla eruzione del 17 Novembre 1843. *Atti Accad Gioenia Sci Nat Catania* 20:225–257
- Giammanco S, Ottaviani M, Valenza M, Veschetti E, Principio E, Giammanco G, Pignato S (1998a) Major and trace elements geochemistry in the ground waters of a volcanic area: Mount Etna (Sicily). *Water Res* 32:19–30, DOI [10.1016/S0043-1354\(97\)00198-X](https://doi.org/10.1016/S0043-1354(97)00198-X)
- Giammanco S, Inguaggiato S, Valenza M (1998b) Soil and fumarole gases of Mount Etna: geochemistry and relations with volcanic activity. *J Volcanol Geotherm Res* 81:297–310, DOI [10.1016/S0377-0273\(98\)00012-2](https://doi.org/10.1016/S0377-0273(98)00012-2)
- Giammanco S, Gurrieri S, Valenza M (1999) Geochemical investigations applied to active fault detection in a volcanic area: the North–East Rift on Mt. Etna (Sicily, Italy). *Geophys Res Lett* 26:2005–2008
- Giammanco S, Ottaviani M, Veschetti E (2007) Temporal variability of major and trace elements concentrations in the groundwaters of Mt. Etna (Italy): effects of transient input of magmatic fluids highlighted by means of cluster analysis. *Pure Appl Geophys* 164:2523–2547, DOI [10.1007/s00024-007-0286-4](https://doi.org/10.1007/s00024-007-0286-4)
- Guest JE, Murray JB, Kilburn CRJ, Lopes RMC, Fidzuk P (1980) An eyewitness account of the Bocca Nuova explosion on 12 September 1979. U.K. Research on Mount Etna, 1977–1979. The Royal Society, London, pp 44–46
- Haeni C (1931) Tätigkeit und Veränderungen am Etna seit dem Ausbruch von 1928 bis Ende 1930. *Zeitsch Vulkanol* 13:245–248
- Harris AJL, Neri M (2002) Volumetric observations during paroxysmal eruptions at Mount Etna: pressurized drainage of a shallow chamber or pulsed supply? *J Volcanol Geotherm Res* 116:79–95, DOI [10.1016/S0377-0273\(02\)00212-3](https://doi.org/10.1016/S0377-0273(02)00212-3)
- Hart K, Carey S, Sigurdsson H, Sparks RSJ, Robertson REA (2004) Discharge of pyroclastic flows into the sea during the 1996–1998 eruptions of the Soufrière Hills volcano, Montserrat. *Bull Volcanol* 66:599–614, DOI [10.1007/s00445-004-0342-1](https://doi.org/10.1007/s00445-004-0342-1)
- Hochstein MP, Browne PRL (2000) Surface manifestations of geothermal systems with volcanic heat sources. In: Sigurdsson H, Houghton BF, McNutt SR, Rymer H, Stix J (eds) *Encyclopedia of volcanoes*. Academic, San Diego, pp 835–855
- IGEPN (Instituto Geofísico, Escuela Politécnica Nacional) (2006) Actividad del Volcán Tungurahua—Agosto de 2006. Available at <http://www.igepn.edu.ec/>
- Kieffer G (1979) L'explosion meurtrière du 12 septembre 1979 de l'Etna. *CR Acad Sci Paris Ser D* 289:1013–1016
- Kieffer G (1982) Les explosions phréatiques et phréatomagmatiques terminales à l'Etna. *Bull Volcanol* 44:655–660, DOI [10.1007/BF02597089](https://doi.org/10.1007/BF02597089)
- Lopez DL, Williams SN (1993) Catastrophic volcanic collapse; relation to hydrothermal processes. *Science* 260:1794–1796, DOI [10.1126/science.260.5115.1794](https://doi.org/10.1126/science.260.5115.1794)
- Martin U, Németh K (2007) Blocky versus fluidal peperite textures developed in volcanic conduits, vents and crater lakes of phreatomagmatic volcanoes in Mio/Pliocene volcanic fields of Western Hungary. *J Volcanol Geotherm Res* 159:164–178, DOI [10.1016/j.jvolgeores.2006.06.010](https://doi.org/10.1016/j.jvolgeores.2006.06.010)
- Mattox TN, Mangan MT (1997) Littoral hydrovolcanic explosions: a case study of lava–seawater interaction at Kilauea Volcano. *J Volcanol Geotherm Res* 75:1–17, DOI [10.1016/S0377-0273\(96\)00048-0](https://doi.org/10.1016/S0377-0273(96)00048-0)
- Morrissey M, Zimanowski B, Wohletz K, Büttner R (2000) Phreatomagmatic fragmentation. In: Sigurdsson H, Houghton BF, McNutt SR, Rymer H, Stix J (eds) *Encyclopedia of volcanoes*. Academic, San Diego, pp 431–445
- Murray JB (1980) The Bocca Nuova: its history and possible causes of the September 1979 explosion. In: Huntingdon AT, Guest JE, Francis EH (eds) *United Kingdom Research on Mount Etna 1977–1979*. The Royal Society, London, pp 46–50
- Murray J, Décobecq D, Bond A (1989–1990) L'éruption paroxysmale du cratère Nord-est de l'Etna du 24 Septembre 1986. *LAVE Bulletin* 22:11–23; 23:5–18; 24:11–21
- Németh K, Martin U (2007) Shallow sill and dyke complex in western Hungary as a possible feeding system of phreatomagmatic volcanoes in “soft-rock” environment. *J Volcanol Geotherm Res* 159:138–152, DOI [10.1016/j.jvolgeores.2006.06.014](https://doi.org/10.1016/j.jvolgeores.2006.06.014)
- Neri M, Acoella V (2006) The 2004–2005 Etna eruption: implications for flank deformation and structural behaviour of the volcano. *J Volcanol Geotherm Res* 158:195–206, DOI [10.1016/j.jvolgeores.2006.04.022](https://doi.org/10.1016/j.jvolgeores.2006.04.022)

- Neri M, Acocella V, Behncke B (2004) The role of the Pernicana fault system in the spreading of Mt. Etna (Italy) during the 2002–2003 eruption. *Bull Volcanol* 66:417–430, DOI [10.1007/s00445-003-0322-x](https://doi.org/10.1007/s00445-003-0322-x)
- Neri M, Acocella V, Behncke B, Maiolino V, Ursino A, Velardita R (2005) Contrasting triggering mechanisms of the 2001 and 2002–2003 eruptions of Mount Etna (Italy). *J Volcanol Geotherm Res* 144:235–255, DOI [10.1016/j.jvolgeores.2004.11.025](https://doi.org/10.1016/j.jvolgeores.2004.11.025)
- Neri M, Behncke B, Burton M, Galli G, Giammanco S, Pecora E, Privitera E, Reitano D (2006) Continuous soil radon monitoring during the July 2006 Etna eruption. *Geophys Res Lett* 33:L24316, DOI [10.1029/2006GL028394](https://doi.org/10.1029/2006GL028394)
- Opfergelt S, Delmelle P, Boivin P, Delvaux B (2006) The 1998 debris avalanche at Casita volcano, Nicaragua: investigation of the role of hydrothermal smectite in promoting slope instability. *Geophys Res Lett* 33:L15305, DOI [10.1029/2006GL026661](https://doi.org/10.1029/2006GL026661)
- Pérez W, Freundt A (2006) The youngest highly explosive basaltic eruptions from Masaya caldera (Nicaragua): stratigraphy and hazard assessment. *Geol Soc Am Spec Pap* 412:189–207, DOI [10.1130/2006.2412\(10\)](https://doi.org/10.1130/2006.2412(10))
- Ponte G (1927) Il vulcarolo sull'Etna e la utilizzazione del suo vapore aqueo. *Boll Accad Gioenia Sci Nat* 57(1–2):14–17
- Reid ME, Sisson TW, Brien DL (2001) Volcano collapse promoted by hydrothermal alteration and edifice shape, Mount Rainier, Washington. *Geology* 29:779–782, DOI [10.1130/0091-7613\(2001\)29<0779:VCPBHA>2.0.CO;2](https://doi.org/10.1130/0091-7613(2001)29<0779:VCPBHA>2.0.CO;2)
- ReliefWeb (2006–2007) Southeast Asia: typhoon dorian—Dec 2006. Available at: <http://www.reliefweb.int/rw/dbc.nsf/doc108?OpenForm&rc=3&emid=TC-2006-000175-PHL>
- Rowe GL, Brantley SL, Fernandez M, Fernandez JF, Borgia A, Barquero J (1992) Fluid-volcano interaction in an active stratovolcano—the crater lake system of Poas volcano, Costa Rica. *J Volcanol Geotherm Res* 49:23–51, DOI [10.1016/0377-0273\(92\)90003-V](https://doi.org/10.1016/0377-0273(92)90003-V)
- Salerno G, Caltabiano T, Burton M, Bruno N, Longo E (2005) Anomalous degassing rates from Mt. Etna, 2001–2005. *Geophys Res Abstr* 7:10606
- Spence R, Kelman I, Brown A, Toyos G, Purser D, Baxter P (2007) Residential building and occupant vulnerability to pyroclastic density currents in explosive eruptions. *Nat Hazards Earth Syst Sci* 7:219–230
- Steiner A (1977) The Wairakei geothermal area, North Island, New Zealand. *N Z Geol Surv Bull* 90:1–136
- Tanguy J-C, Ribière C, Scarth A, Tjetjep WS (1998) Victims from volcanic eruptions: a revised database. *Bull Volcanol* 60:137–144, DOI [10.1007/s004450050222](https://doi.org/10.1007/s004450050222)
- Taylor GA (1963) Seismic and tilt phenomena preceding a Pelean type eruption from a basaltic volcano. *Bull Volcanol* 26:5–11, DOI [10.1007/BF02597269](https://doi.org/10.1007/BF02597269)
- Ui T, Takarada S, Yoshimoto M (2000) Debris avalanches. In: Sigurdsson H, Houghton BF, McNutt SR, Rymer H, Stix J (eds) *Encyclopedia of volcanoes*. Academic, San Diego, pp 617–626
- Valentine GA, Fischer RV (2000) Pyroclastic surges and blasts. In: Sigurdsson H, Houghton BF, McNutt SR, Rymer H, Stix J (eds) *Encyclopedia of volcanoes*. Academic, San Diego, pp 571–580
- Vallance JW (2000) Lahars. In: Sigurdsson H, Houghton BF, McNutt SR, Rymer H, Stix J (eds) *Encyclopedia of volcanoes*. Academic, San Diego, pp 601–616
- Wehrmann H, Bonadonna C, Freundt A, Houghton BF, Kutterolf S (2006) Fontana Tephra: a basaltic Plinian eruption in Nicaragua. *Geol Soc Am Spec Pap* 412:209–223, DOI [10.1130/2006.2412\(11\)](https://doi.org/10.1130/2006.2412(11))
- White JDL (2006) Impure coolants and interaction dynamics of phreatomagmatic eruptions. *J Volcanol Geotherm Res* 74:155–170, DOI [10.1016/S0377-0273\(96\)00061-3](https://doi.org/10.1016/S0377-0273(96)00061-3)
- White JDL, Houghton B (2000) Surtseyan and related phreatomagmatic eruptions. In: Sigurdsson H, Houghton BF, McNutt SR, Rymer H, Stix J (eds) *Encyclopedia of volcanoes*. Academic, San Diego, pp 495–511
- White JDL, Houghton B (2006) Primary volcanoclastic rocks. *Geology* 34:677–680, DOI [10.1130/G22346.1](https://doi.org/10.1130/G22346.1)
- White JDL, Schmincke H-U (1999) Phreatomagmatic eruptive and depositional processes during the 1949 eruption on La Palma (Canary Islands). *J Volcanol Geotherm Res* 94:283–304, DOI [10.1016/S0377-0273\(99\)00108-0](https://doi.org/10.1016/S0377-0273(99)00108-0)
- Witham CS (2005) Volcanic disasters and incidents: a new database. *J Volcanol Geotherm Res* 148:91–233, DOI [10.1016/j.jvolgeores.2005.04.017](https://doi.org/10.1016/j.jvolgeores.2005.04.017)
- Wohletz KH (1986) Explosive magma–water interactions: thermodynamics, explosion mechanisms, and field studies. *Bull Volcanol* 48:245–264, DOI [10.1007/BF01081754](https://doi.org/10.1007/BF01081754)
- Yamamoto T, Takarada S, Suto S (1993) Pyroclastic flows from the 1991 eruption of Unzen volcano, Japan. *Bull Volcanol* 55:166–175, DOI [10.1007/BF00301514](https://doi.org/10.1007/BF00301514)
- Zimanowski B, Büttner R (2002) Dynamic mingling of magma and liquefied sediments. *J Volcanol Geotherm Res* 114:37–44, DOI [10.1016/S0377-0273\(01\)00281-5](https://doi.org/10.1016/S0377-0273(01)00281-5)
- Zimbelman DR, Watters RJ, Firth IR, Breit GN, Carrasco-Nuñez G (2004) Stratovolcano stability assessment methods and results from Citlaltépetl, Mexico. *Bull Volcanol* 66:66–79, DOI [10.1007/s00445-003-0296-8](https://doi.org/10.1007/s00445-003-0296-8)